Simulating space and time dependence of a simplified thorium cycle in a Molten Salt Fast Reactor

Hartog, T.

BSc End Project

TU Delft

Delft, August 26, 2021

Supervisors:
Danny Lathouwers
Jan Leen Kloosterman

Abstract

This thesis aims to demonstrate how the fuel composition of a Molten Salt Fast Reactor changes over time and space by modeling fuel transport in the primary circuit of the reactor. Numerous variables, such as the density of the various nuclides in the fuel and the amount of energy generated by the system, were considered in different simulated models. This thesis discusses the theory required to perform temporal and spatial simulation of fuel composition, including how specific nuclides can transmute into other nuclides and how fuel is carried through the reactor system.

The explicit Euler method was used to model time dependence of the fuel composition, which included two different time scales for the two primary components of the system equation. Using the smaller time scale which is relevant to convection, a scaling issue arose due to the extensive time span covered by the system.

Because of this, two separate simulation were performed. The first without a convection term, where all the nuclides from the simplified thorium fuel cycle were present. This model gave an accurate representation of the change in fuel composition. The second a simplified system using fictional nuclides based on the simplified thorium fuel cycle that was created to demonstrate the code's capability of simulating fuel transport through the system. As of now, the code responsible for the simulation of convection is highly inefficient and takes a long time to calculate. Further research would improve these convection calculations, simulate the production of fission products and implement perturbation theory to further improve the model.

Contents

1. Introduction

In the quest for clean and cheap energy, massive solar and wind farms have sprung up worldwide. Investments in these renewable resources reached 282.2 billion dollars in 2019. Include the last nine years, and that figure reaches 2.7 trillion dollars. [1] This is good news for the decarbonization of the energy industry. However, this raises the question: why is there so much less focus on nuclear energy?

A good measure for comparing the success in low-carbon energy production of different countries is their carbon dioxide output per kilowatt-hour of produced energy.
68% of France's electricity generation comes from nuclear, producing only 44 grams of carbon dioxide for every kWh produced. On the other hand, Germany is gradually closing down all of its nuclear power plants and replacing them with wind energy and natural gas plants and produces 373 grams of carbon dioxide for every kilowatt-hour. This is a clear indication of France performing better than Germany, so why does Germany continue to invest billions of dollars into wind turbines instead of nuclear power plants? [2]
It is interesting to note that several countries are phasing out nuclear energy in favor of fossil fuels and renewable energy. To understand why this is the case, we must address multiple factors. Consider the following: nuclear reactor waste is radioactive and must be safely stored for an extended time. Additionally, social and political variables, such as public opinion on nuclear power due to the Fukushima and Chernobyl incidents and the fear of nuclear proliferation, play a role. Economic considerations include whether or not the possible financial gain out-weights the time and energy required to obtain a return on investment. However, technological improvements will likely enable the construction of nuclear reactors that are safer, more sustainable, more efficient, and more affordable. Some of these technological improvements entail will be discussed in this thesis. But first, a quick overview of the workings of a reactor will be given below

Central to the nuclear power plant is the core, a bound region in which atomic nuclei fission and decay, where neutron multiplication occurs and chain reactions follow. As atomic nuclei fission and break apart into lighter nuclides, energy is released that can be used to generate electricity. As this process continues, a variety of nuclei accumulate within the core. It is vital to monitor the composition of the nuclei density in the core to ensure the optimal operation of the powerplant as some of the generated nuclei may interfere with the reactor's correct operation.

1.1 Aim and Layout of the thesis

This thesis aims to simulate a simplified thorium fuel cycle in a Molten Salt Fast Reactor over time and space. Several chapters have been written that go through the whole process to achieve this. Starting with a list of essential definitions, followed by a chapter on the theory of Molten

Salt (Fast) Reactors and how the fuel within said reactors can change over time and throughout the system. Then, a chapter on the methodology is presented in which a detailed description of the computational tool developed will be given, with some of the problems that were solved along the way. After this, a chapter on the simulated results is delivered and discussed. Ending with a conclusion.

2. Theory

2.1 Molten Salt Reactor

Molten salt reactors (MSRs) operate at low pressure using molten fluoride salts as the primary coolant. This is not a radical departure from previous reactor designs using solid fuel. However, extending this idea to the inclusion of fissile and fertile fuel in salt marks a jump in lateral thinking compared to almost every reactor run to date. The idea is, however, not a novel one. MSRs are capable of operating with either thermal or fast neutrons and a variety of fuels. Much of the current interest in the MSR concept is focused on the use of thorium to breed fissile uranium-233. There are numerous MSR design possibilities and many interesting issues associated with their commercialization, particularly with thorium. The salts used as primary coolants, mostly lithium-beryllium fluoride and lithium fluoride, remain liquid and stable without pressurization between around 500°C to approximately 1400°C, in stark contrast to a Pressurised Water Reactor, which operates at approximately 315°C at 150-atmosphere pressure. Because of the MSR's higher operating temperatures (around 700 degrees Celsius [3]), electricity is generated more efficiently.

A molten salt reactor (MSR) is a type of nuclear fission reactor in which the primary coolant and fuel are made of molten salt. Thorium, uranium, and plutonium all make for suitable fluoride salts that dissolve quickly in the LiF mixture, and thorium and uranium may be easily separated from each other when bounded to a fluoride making easier reprocessing. Additionally, an MSR has the advantage of homogeneous fuel irradiation and the ability to reload and process fuel online or in batches without the need for reactor shutdown and the transfer of tiny amounts of fuel.

There are two main types of nuclear reactors. A thermal nuclear reactor is a reactor in which thermal neutrons initiate the fission reaction. These neutrons maintain thermal equilibrium with the molecules surrounding them and have a kinetic energy of 0.025 eV. Such neutrons have a high possibility of triggering a fission reaction in heavy nuclides. Each fission reaction generates between one and seven fast neutrons, but on average about three. This fast neutron has far higher energy compared to a thermal neutron, and its energy can range anywhere between 1 and 10 MeV. Because fast neutrons have a low probability of interacting with a nuclide, they cannot continue a chain reaction with low enriched fuel. As a result, there are two possible ways to continue chain reactions: decreasing the velocity of neutrons generated during fission or increasing the enrichment of the fuel.

In thermal reactors, low-enriched fuel is employed, and hence a moderator such as water, graphite, or other material is used to slow down the neutrons created during the fission reaction. Fast reactors work without moderators. To compensate for the reduction in the fission probability

of fast neutrons caused by heavy nuclides, relatively high enriched fuel (15–20 %) is required. Thus, in both types of reactors, the chain reaction continues.

Looking at the schematic of the MSR figure 1, it can be seen that the system consists of three loops. The primary loop contains radioactive molten salt. This salt serves two purposes: nuclear fuel and the primary coolant in the system. As the fissile material in the fuel undergoes fission in the core, highly energetic fission fragments are produced. They slow down as a result of collisions with neighboring atoms, so they lose energy. This is the primary method by which fission energy is converted to heat in the fuel. This heat is transferred through the primary heat exchanger to a secondary loop in which non-radioactive molten salt flows. This salt acts as a heat exchange system between the primary and tertiary loops. In this third loop, electricity is generated using steam turbines, often through a Rankine cycle.

A significant advantage of using liquid fuel can be seen when the fuel composition change is noted over time. As the heavy nuclides initially present in the fuel capture neutrons, they transform through a nuclear chain reaction into other actinides. After absorption of a neutron, they may fission, breaking apart into lighter fission products that can affect the reactor's performance in various ways. Some fission products and actinides, for example, may be able to absorb neutrons, effectively halting the nuclear chain process required to keep fission going in the core and maintaining criticality. This holds for all nuclear power plants. On the other hand, traditional solid-fuel reactors must be shut down to replace spent fuel assemblies, refuel the reactor with new fuel, and remove the poisons. A chemical processing facility enables the MSR to process its fuel continuously, allowing for the continual operation of the reactor.

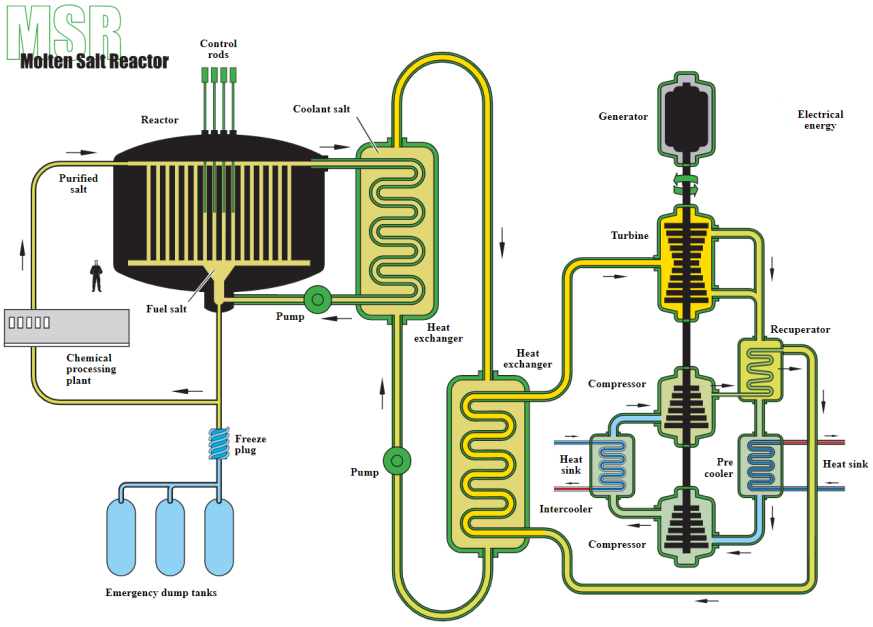

Figure 1: Molten Salt Reactor schematic

By approximation, there only is a significant neutron flux in the core of an MSR. As a result, it is the only place where fission occurs and where heat is produced. For a reactor to operate

steady state, all heat generated in the system must be removed as soon as it is generated. The heat transfer rate must be equal to or higher than the heat generation rate; otherwise, the fission reactions will stop. The control rods depicted in Figure 1 can be inserted into the reactor core to inhibit additional fissions by absorbing neutrons. Control rods are a critical component of a nuclear reactor's safety system since they are responsible for maintaining the reactor's desired frequency of fission reactions.
The MSR has a freeze plug as a full passive safety measure. In the primary loop, a freeze plug is used, as shown in Figure 1. This is a valve plugged with frozen fluoride salt that is actively cooled by air. If the power supply fails, the airflow stops, and the salt will melt in 15 minutes [4], causing the entire contents of the reactor to drain into the emergency dump tanks below. The fission chain reaction comes to a halt here, and the fuel is cooled by natural convection.

2.1.1 Molten Salt Fast reactor

Many of the thermal MSR functions and the Molten Salt Fast Reactor (MSFR) are analogous. Because the MSFR does not use a solid moderator, there are no concerns about the erosion of the graphite moderators. This results in a fast spectrum breeder reactor that can be operated on a thorium fuel cycle. Fast breeder reactors are a subset of fast reactors. Since fast reactors frequently have an excess of neutrons due to low parasitic absorption, they can be used to "breed" more fuel from otherwise fertile isotopes.

The Generation IV International Forum (GIF) is an initiative currently researching a set of nuclear reactor designs that significantly improves upon prior reactor designs. The initiative selected the MSFR idea as a candidate for GEN IV in 2008. The reference MSFR is a 3 GW [5] reactor operating at a maximum fuel salt temperature of 750°C, and a total fuel salt volume of 18 m^3 in the primary circuit [5].

Under typical operating conditions, the fuel salt travels up from the bottom to the top of the core and through the 16 fuel loops, as illustrated in Figure 2. Each of these fuel loops is equipped with a pump, a heat exchanger, and a bubbling system [5].

The fuel salt is a Mixed Oxide Fuel (MOX) composed of 77.5% lithium fluoride, 20% Thorium tetra-fluoride and 2.5% Uranium tetra-fluoride [6]. More details can be found in the appendix in Table 2.

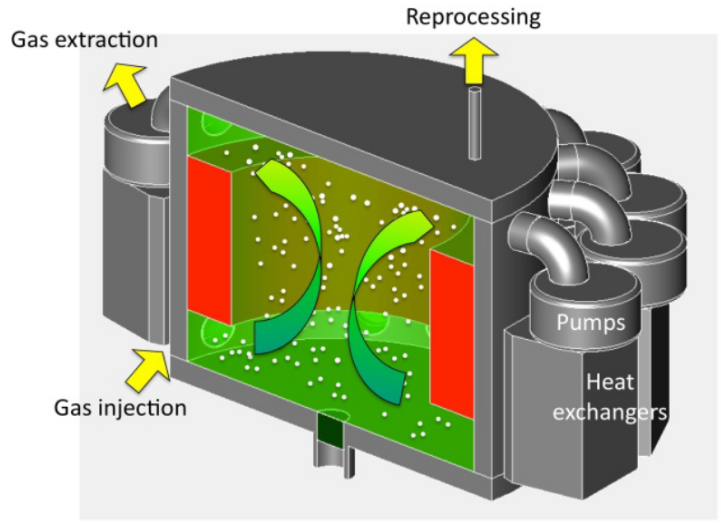

Figure 2: Illustration of a three-dimensional layout for the Molten Salt Fast Reactor (MSFR)

Additionally, control rods or neutron poisons are not required to manage criticality, as the strong negative feedback coefficients enable reactivity control based on the balance of power generated in the fuel salt and power extracted by the heat exchangers. The elimination of control rods simplifies reactor operation, and with fewer moving parts, the potential of accidents is decreased.

2.2 Nuclear Reactor Physics

2.2.1 Nuclear Reactions

Atomic nuclei are made up of neutrons and protons attracted to one other by the strong nuclear force, and the protons are repelled via the electromagnetic force. The nuclei are stabilized by neutrons, which counteract the protons' repulsion. As a result, the ratio of neutrons to protons will grow as the mass of the nuclide increases. Also, because neutrons follow the Pauli exclusion principle, there cannot be too many or too few neutrons in a nucleus for any given quantity of protons. Because of this balance of repulsion and attraction, only a few combinations can form stable nuclei. If a nuclide is unstable, it will decay. Because unstable nuclides decay through radioactive decay pathways, it makes sense to consider the fact that in nature, primarily stable nuclides can be found as most of the the unstable nuclides have decayed away. Explaining all of the possible nuclear reactions does not contribute to the thesis's goal. Parts will be simplified or omitted in order to focus on the essential aspects.

One of the ways a nuclide can transform is through β^- decay. When this happens, a parent nuclide disintegrates into a daughter nuclide when a neutron turns into a proton. This way, the nuclide maintains its atomic weight but changes into a different element.

The half-life $t_{\frac{1}{2}}$ is used to determine how much of a certain nuclide decays over a certain time-span and can be related to a decay constant λ as:

$$\lambda = \frac{ln(2)}{t_{\frac{1}{2}}} \tag{1}$$

This decay constant λ is used in the following equation to determine the rate of change for a certain nuclide 'k' due to spontaneous nuclear decay:

$$\frac{dC_k}{dt} = -\lambda_k C_k(t) \tag{2}$$

In this equation C_k is the amount of nuclides of type 'k' per unit volume and λ_k the decay rate corresponding to that nuclide type. To also calculate the change in density C_k as a result of another nuclide (say 'l') decaying into 'k' the equation can be extended as:

$$\frac{dC_k}{dt} = -\lambda_k C_k(t) + \sum_l \lambda_{l\to k} C_l \tag{3}$$

In this equation, the sum over 'l' gives the different types of nuclides' l' that change into 'k'. These are two of the more common types of decay and ways through which nuclides can change into other nuclides. Another meaningful way this can happen involves the collision between a neutron and a nuclide. As can be seen in Figure 3, when a neutron with a sufficient amount of energy collides with a nuclide, there are a couple of things that can happen:
After a neutron-nucleus interaction, a target nucleus emits a single neutron known as a neutron scattering reaction. There is no energy transmitted into the nuclear excitation of the target nucleus in an elastic scattering reaction.
In an inelastic scattering process involving a neutron and a target nucleus, some of the incident neutron's energy is absorbed by the recoiling nucleus, and the nucleus remains excited. A neutron emission reaction can occur where a neutron is ejected with lower kinetic energy than the incident neutron. Depending on the kinetic energy of the incident neutron, more than one neutron can be ejected from the nuclide. These are referred to as $(n, 2n)$, $(n, 3n)$, $(n, 4n)$, etc. reactions.

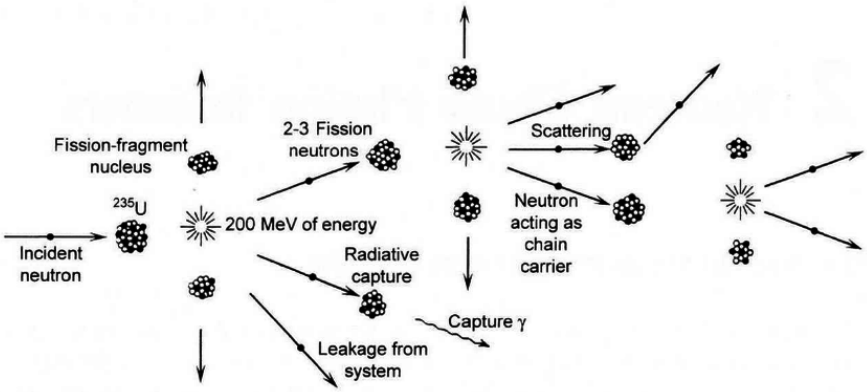

Figure 3: Neutron chain fission reaction process example for a Uranium-135 nuclide

As a neutron is absorbed in a neutron absorption reaction, the nuclide reaches an excited state, resulting in the formation of a compound nucleus. The nuclide usually loses its excess energy through radiative capture (denoted by σ_γ), in which it emits gamma radiation.

There is a chance that a neutron-induced fission reaction will occur if the nuclide is fissionable. If it does, two or more fission products along with thermal energy and some neutrons are produced. The reactor reaches criticality when each fission event releases enough neutrons to sustain more fission events. As a result, the reactor is said to be critical.

2.2.2 Microscopic Cross Sections

To determine the probability of any of the reactions mentioned previously, the microscopic cross-section and the neutron flux density must be considered. The neutron flux density is the total number of neutrons passing through a unit cross-section in all directions per unit time. The cross-section of a nuclide at the microscopic level is the effective target area for an incoming neutron.

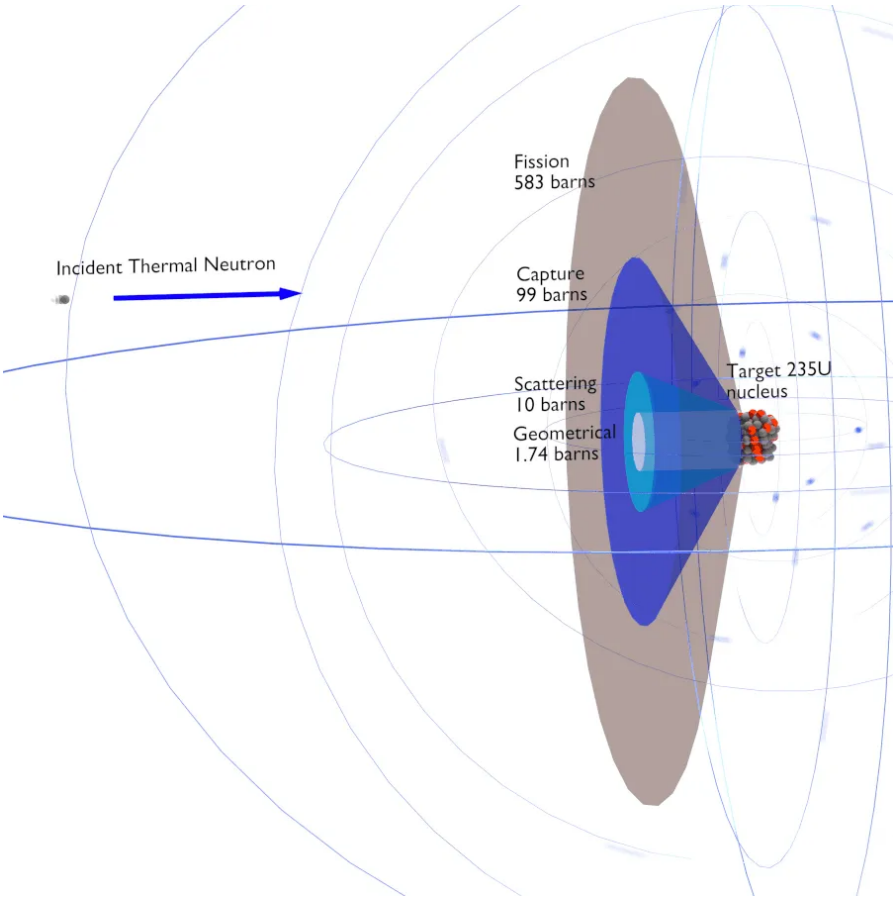

Figure 4: Microscopical cross-sections of uranium-235 and an incident thermal neutron.

As illustrated in Figure 4, due to quantum tunneling, the microscopic cross-section of nuclides does not have to correspond to their geometrical cross-section. Interestingly, thermal neutrons have a greater chance than fast neutrons of initiating a neutron-nucleus interaction. The neutron cross-section is a combination of the scattering σ_s, radiative capture σ_γ, and fission σ_f cross-sections shown in Figure 4. These cross-sections all have different values for different neutron energies and neutron types. If the neutron capture reaction for a particular nuclide requires a

large amount of energy to occur, the cross-section for higher energy neutrons will be larger than those for lower energy neutrons.
The rate of change for a certain nuclide 'k' due to neutron absorption is given by the following formula:

$$\frac{dC_k}{dt} = \phi(r,t)(-\sigma^k C_k + \sum_l \sigma^{l\to k} C_l) \tag{4}$$

In this equation, $\Phi(r,t)$ is the neutron flux density which is now taken to be dependent of time but later will be estimated to only depend on position within the system. σ^k is the cross-section that contributes to the loss of nuclides' k' and $\sigma^{(l\to k)}$ is the cross-section that contributes to the increase of nuclides 'k' from other nuclides 'l'. For the sake of readability in the following equations, the sub-scrips that give the type of absorption reaction for the corrections have been omitted.

2.2.3 Production term

By combining Equations 3 and 4, the change in density of nuclide 'k' over time can be found as a production term:

$$\frac{dC_k}{dt} = -C_k(t)(\lambda_k + \phi(r,t)\sigma^k) + \sum_l C_l(t)(\lambda_{l\to k} + \phi(r,t)\sigma^{l\to k}) \tag{5}$$

The first term on the RHS indicates the decrease in the nuclide 'k' caused by beta decay and neutron absorption. The second term on the right indicates the increase in the nuclide 'k' due to the decay of many different nuclides 'l' that undergo beta minus decay and neutron absorption. The change in a single nuclide can now be calculated. To calculate the change in multiple nuclides, Equation 5 can be expanded into a system of equations:

$$\frac{d\mathbf{C}(t)}{dt} = P\mathbf{C}(t) \tag{6}$$

In this equation, $\mathbf{C(t)}$ is a vector containing the densities of the fuel's nuclides. P is a time-independent matrix representing the change in nuclide densities resulting from neutron absorption and decay. Equation 6 can be expanded to provide a complete understanding of its operation:

$$\mathrm{d}_{\overline{dt}}\begin{bmatrix} C_1 \\ C_2 \\ \vdots \\ C_k \end{bmatrix} = \begin{bmatrix} -\lambda_1 - \phi\sigma^1 & \lambda_{2\to1} + \phi\sigma^{2\to1} & \cdots & \lambda_{k\to1} + \phi\sigma^{k\to1} \\ \lambda_{1\to2} + \phi\sigma^{1\to2} & -\lambda_2 - \phi\sigma^2 & \cdots & \lambda_{k\to2} + \phi\sigma^{k\to2} \\ \vdots & \vdots & \ddots & \lambda_{k\to3} + \phi\sigma^{k\to3} \\ \lambda_{1\to k} + \phi\sigma^{1\to k} & \lambda_{2\to k} + \phi\sigma^{2\to k} & \lambda_{3\to k} + \phi\sigma^{3\to k} & -\lambda_k - \phi\sigma^k \end{bmatrix} = \begin{bmatrix} C_1 \\ C_2 \\ \vdots \\ C_k \end{bmatrix} \tag{7}$$

Consider a single nuclide C_k; with the previous equation, it is now readily apparent how its density varies over time as a function of the other nuclides. This way, the system can be modeled to accommodate any number of nuclides used in a nuclear reactor.

2.3 Fuel transport

To accurately model and predict the changes in the fuel salt within the reactor, the fuel transport must also be considered. The system segments through which a fluid flows are shown in Figure

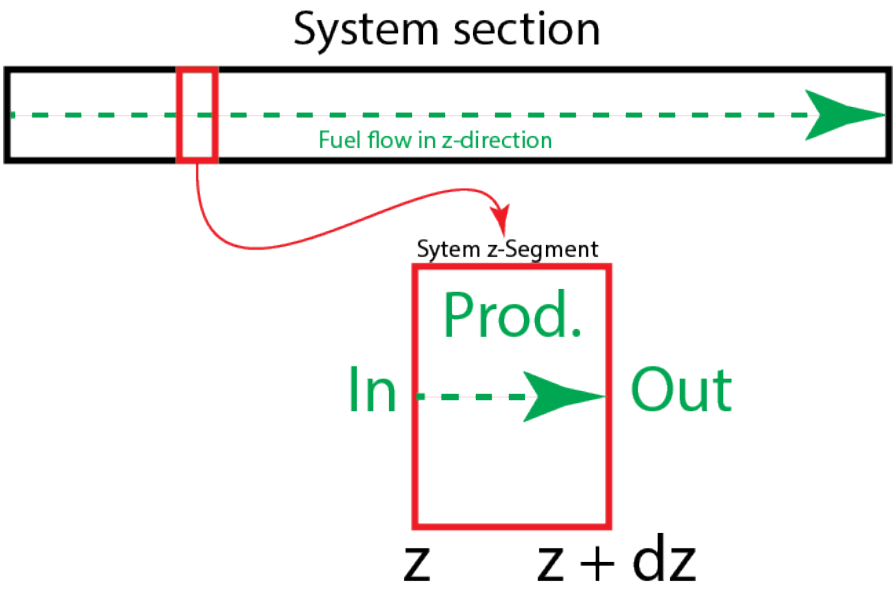

Figure 5: Geometrical model of a segment of a system section illustrating material inflow/outflow and production within the segment.

5. It demonstrates how the convection term is derived. The transport of the various nuclides in the system can be modeled using these segments.
The section is discretized into segments of length Δz, for which the change in nuclide density can be calculated as $In - Out + Production$, where In represents the concentration of nuclides flowing into the segment at position z, Out represents the concentration of nuclides flowing out of the segment at position $z + \Delta z$, and $Production$ describes the way the nuclide composition changes during decay.

The rate of change of a particular nuclide 'k' through a segment is calculated as follows:

$$\frac{dC_z}{dt} = g(t)C(t)_k|_z - g(t)C(t)_k|_{z+dz} + r_k V \tag{8}$$

The first term on the right adds the flow rate $g(t)$ times the density of nuclide 'k' at position z. The second term on the right subtracts the flow rate $g(t)$ times the density of nuclide 'k' at position $z + \Delta z$. The last term, $r_k V$, multiplies the production, which is given by Equation 5, with the volume of the segment, which is given by the $Area$ of the system segment multiplied with Δz.

Dividing the volume out of Equation 8 and excluding the last term $r_k V$ leaves the convection term of the nuclide density in the system:

$$\frac{dC_{k,j}}{dt} = \frac{g(t)}{A_j \Delta z}(C_{k,j} - C_{k,j-1}) \tag{9}$$

With $C_{k,j}$ denoting the density of nuclide 'k' at position j in the system, $g(t)$ the flow of the system which is taken as a constant in the rest of this thesis, A_j the areal cross section of the segment at position j.

This can be expanded into a system of equations which are able to calculate the transport for multiple nuclides:

$$\frac{d\mathbf{C}_{k,j}}{dt} = T\mathbf{C}_{k,j} \tag{10}$$

Where T is a time independent transport matrix that, for each time step, calculates the current position j from the past position $j-1$ for each nuclide k. Equation 10 will be expanded for a single nuclide to illustrate the workings:

$$\mathrm{d}\frac{}{dt}\begin{bmatrix} C_{1,1} \\ C_{1,2} \\ C_{1,3} \\ \vdots \\ C_{1,j} \end{bmatrix} \begin{bmatrix} -\frac{g(t)}{A_1\Delta z} & 0 & 0 & \cdots & \frac{g(t)}{A_1\Delta z} \\ \frac{g(t)}{A_2\Delta z} & -\frac{g(t)}{A_2\Delta z} & 0 & \cdots & 0 \\ 0 & \frac{g(t)}{A_3\Delta z} & -\frac{g(t)}{A_3\Delta z} & \cdots & 0 \\ \vdots & \vdots & \vdots & \ddots & 0 \\ 0 & 0 & 0 & \frac{g(t)}{A_j\Delta z} & -\frac{g(t)}{A_j\Delta z} \end{bmatrix} = \begin{bmatrix} C_{1,1} \\ C_{1,2} \\ C_{1,3} \\ \vdots \\ C_{1,j} \end{bmatrix} \tag{11}$$

The transport of a single nuclide through the system is calculated here for a single time step. For example, consider the nuclide $C_{1,1}$ in the top left, whose transport throughout the system is determined by its position in the current segment and its position in the previous segment.

2.4 Formal Solution

The complete space dependent burn-up equation is created by plugging Equation 5 into Equation 8 such that:

$$\frac{dC_{k,j}}{dt} = \frac{g(t)}{A_j\Delta z}(C_{k,j} - C_{k,j-1}) - C_{k,j}(t)(\lambda_k + \phi_j\sigma^k) + \sum_l C_{l,j}(t)(\lambda_{l\to k} + \phi_j\sigma^{l\to k}) \tag{12}$$

Now the decrease and increase of every nuclide are accounted for at each segment at each time step.

$$\frac{d\mathbf{C}_{k,j}}{dt} = M\mathbf{C}_{k,j} \tag{13}$$

Here, M is a time-independent matrix that calculates the change in multiple nuclides at different points along with the system's segments over time.

M is created as a square matrix with dimensions equal to the number of segments in the system multiplied by the number of distinct nuclei. How the matrix is constructed is illustrated below. Some substitutions are made to maintain readability, such as

The convective term $\frac{g(t)}{A_j\Delta z}$, at a specific position in the system 'j', is substituted by G_j.

The reactive terms, $(\lambda_k + \phi_j\sigma^k)$ and $\sum_l C_{l,j}(t)(\lambda_{l\to k} + \phi_j\sigma^{l\to k})$ from Equation 5 have been replaced with $\beta_{k,j}$ and $\alpha_{l\to k,j}$ respectively. To give the change in nuclide 'k' at position 'j'.

$$\frac{d}{dt}\begin{bmatrix} C_{1,1} \\ C_{2,1} \\ C_{3,1} \\ C_{1,2} \\ C_{2,2} \\ C_{3,2} \\ C_{1,3} \\ C_{2,3} \\ C_{3,3} \\ C_{1,4} \\ C_{2,4} \\ C_{3,4} \end{bmatrix} = \begin{bmatrix} -G_1-\beta_{1,1} & \alpha_{2\to1,1} & \alpha_{3\to1,1} & 0 & 0 & 0 & 0 & 0 & 0 & G_1 & 0 & 0 \\ \alpha_{1\to2,1} & -G_1-\beta_{2,1} & \alpha_{3\to2,1} & 0 & 0 & 0 & 0 & 0 & 0 & 0 & G_1 & 0 \\ \alpha_{1\to3,1} & \alpha_{2\to3,1} & -G_1-\beta_{3,1} & 0 & 0 & 0 & 0 & 0 & 0 & 0 & 0 & G_1 \\ G_2 & 0 & 0 & -G_2-\beta_{1,2} & \alpha_{2\to1,2} & \alpha_{3\to1,2} & 0 & 0 & 0 & 0 & 0 & 0 \\ 0 & G_2 & 0 & \alpha_{1\to2,2} & -G_2-\beta_{2,2} & \alpha_{3\to2,2} & 0 & 0 & 0 & 0 & 0 & 0 \\ 0 & 0 & G_2 & \alpha_{1\to3,2} & \alpha_{2\to3,2} & -G_2-\beta_{3,2} & 0 & 0 & 0 & 0 & 0 & 0 \\ 0 & 0 & 0 & G_3 & 0 & 0 & -G_3-\beta_{1,3} & \alpha_{2\to1,3} & \alpha_{3\to1,3} & 0 & 0 & 0 \\ 0 & 0 & 0 & 0 & G_3 & 0 & \alpha_{1\to2,3} & -G_3-\beta_{2,3} & \alpha_{3\to2,3} & 0 & 0 & 0 \\ 0 & 0 & 0 & 0 & 0 & G_3 & \alpha_{1\to3,3} & \alpha_{2\to3,3} & -G_3-\beta_{3,3} & 0 & 0 & 0 \\ 0 & 0 & 0 & 0 & 0 & 0 & G_4 & 0 & 0 & -G_4-\beta_{1,4} & \alpha_{2\to1,4} & \alpha_{3\to1,4} \\ 0 & 0 & 0 & 0 & 0 & 0 & 0 & G_4 & 0 & \alpha_{1\to2,4} & -G_4-\beta_{2,4} & \alpha_{3\to2,4} \\ 0 & 0 & 0 & 0 & 0 & 0 & 0 & 0 & G_4 & \alpha_{1\to3,4} & \alpha_{2\to3,4} & -G_4-\beta_{3,4} \end{bmatrix} \begin{bmatrix} C_{1,1} \\ C_{2,1} \\ C_{3,1} \\ C_{1,2} \\ C_{2,2} \\ C_{3,2} \\ C_{1,3} \\ C_{2,3} \\ C_{3,3} \\ C_{1,4} \\ C_{2,4} \\ C_{3,4} \end{bmatrix}$$

Figure 6: Complete Burn-up Matrix

The workings of the complete burn-up matrix are illustrated in the example given in Figure 6 below. Here a matrix is created for a system with three nuclides divided into four z-segments. Over the diagonal, the production matrices from Equation 7 calculate the change in the concentration of a particular nuclide at a particular z-segment in the system. In conjunction with the convection terms, these production terms can account for the position and change of each nuclide over time.

2.5 Thorium Fuel Cycle

A naturally occurring element with the atomic number 90 is thorium. The element is estimated to be three times more abundant than uranium. It has seven unstable isotopes, with only one of them (Th-232) being relatively stable, having a half-life of around 14 billion years. Much longer than the other Isotopes making it nearly the only isotope found naturally. The different types of nuclides in a thorium cycle can be subdivided into three groups:

Fissionable nuclides are nuclides capable of nuclear fission after capturing either a fast or thermal neutron. Some typical fissionable materials: ${}^{239}_{94}Pu$, ${}^{240}_{94}Pu$, ${}^{241}_{94}Pu$ and ${}^{233}_{92}U$, ${}^{235}_{92}U$, ${}^{238}_{92}U$.

Fissile nuclides, a subset of fissionable nuclides, are nuclides capable of nuclear fission only after capturing a thermal neutron. ${}^{238}_{92}U$ is not fissile where ${}^{233}_{92}U$ and ${}^{235}_{92}U$ are for example.

Fertile nuclides. These nuclides cannot undergo fission by thermal neutrons but can be transformed into fissile nuclides through neutron capture-induced decay. Examples are ${}^{238}_{92}U$ and ${}^{232}_{90}Th$. The thorium cycle is a nuclear chain process in which fertile ${}^{232}_{90}Th$ absorbs a neutron, and through a cascade of nuclear decay reactions, transforms into the fissile ${}^{233}_{92}U$ as shown in Figure 7.

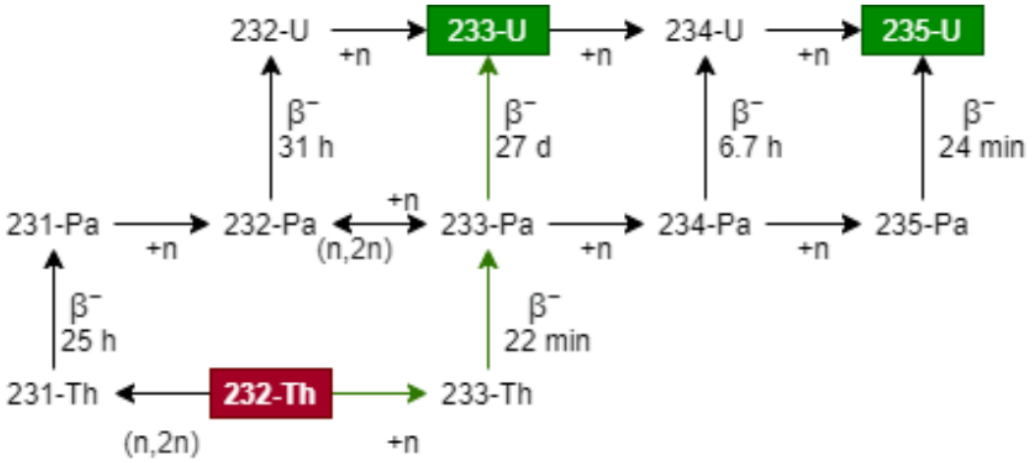

Figure 7: A simplified thorium fuel cycle. Fertile ${}^{232}_{90}Th$ converts via many decay reactions to fissile ${}^{233}_{92}U$ and ${}^{235}_{92}U$.

The arrows pointing to the right in Figure 7 represent a neutron's absorption, which increases the atomic weight. The upward arrows depict β^- decay along with the corresponding half-life, maintaining the same atomic weight but increasing the number of protons. The arrows pointing to the left illustrate a (n,2n) reaction, which results in the loss of a single neutron. The actual fuel cycle is more complex but has been simplified to not divert from the purpose of this thesis.

2.5.1 Fission Products

Fission of a parent nuclide produces two (rarely three) fission products along with some fast neutrons. It is impossible to determine beforehand the types of fission products created in each fission process. However, the distribution of fission products can be determined over a large number of fission reactions, as illustrated in Figure 8.

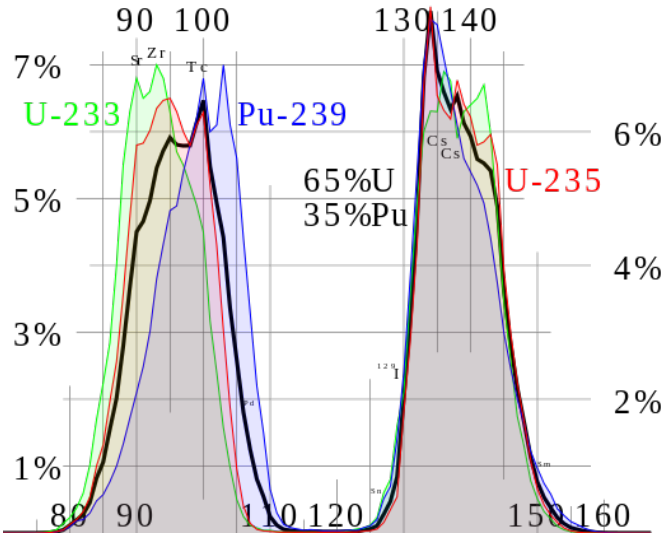

Figure 8: Thermal neutron fission product yields by mass for uranium-235, plutonium-239, and uranium-233 which is utilized in the thorium cycle.

The yield of an isotope gives the number of isotopes produced per fission. Here this is given as the number of fission products created per fission event for a particular nuclide.

2.5.2 Poisons

A poison (alternatively referred to as a neutron absorber or a nuclear poison) is a material with a large cross-section for neutron absorption. Absorbing neutrons is typically an unwanted effect in these applications. However, neutron-absorbing materials, sometimes referred to as poisons, are deliberately injected into certain reactors to lessen the high reactivity of their initial new fuel load. While some of these poisons concentrations diminish as neutrons are absorbed during the reactor operation, others remain relatively constant. An example of a neutron poison is ${}^{135}_{54}Xe$ with a macroscopic cross-section of around 2.6 billion barns [7] for a thermal neutron. Compared to the cross-section of 99 barns [8] for ${}^{235}_{92}U$. Moreover, it is easy to see why xenon has such a tremendous impact on the operation of a nuclear reaction.

2.5.3 Chemical Processing

Poisons are removed, and new fuel is introduced to keep the MSR operating at peak efficiency. This can be accomplished either within the core or through the use of an external chemical processing unit. Fluorination is one method for achieving this outside of the core. Fission products and actinides combine with fluoride within the fuel to form a salt. Due to their distinct boiling points, these salts can be separated via fractional distillation [9]. The undesirable nuclides are separated from the cleaned fuel before reintroduction into the reactor.

Helium bubbling is another method for removing specific nuclides. This removal is accomplished within the core. At the bottom of the core in Figure 2, helium is introduced. The helium is propelled upward by buoyant forces through the core, where specific nuclides bind to it (Xenon being the most important). At the top of the reactor, the gas is separated from the liquid, and the bound nuclides are removed.

3. Methodology

This chapter establishes, models, and simulates the MSFR geometry. To accomplish this, data from an MSR obtained from [4] is employed. The techniques developed for this reactor will be extended to the MSFR. After that, the neutron density flux shape and weight of the reactor will be discussed. The implementation of this into Python is then explained, after which the problems and solutions with the simulation of the data are considered and finally, the model's uncertainties are discussed.

3.0.1 MSFR Model Geometry

In Figure [9], a cross-section of the core is illustrated schematically. The computational tool models the MSFR core as a cylindrical structure with a radius of 112.75 cm and a height of 225.5 cm. The fuel composition is considered to be homogeneous within the core, which has a volume of 18 m^3 [5]. Half of the salt volume is contained within the core, while the remaining is contained within the fuel loops outside the core.

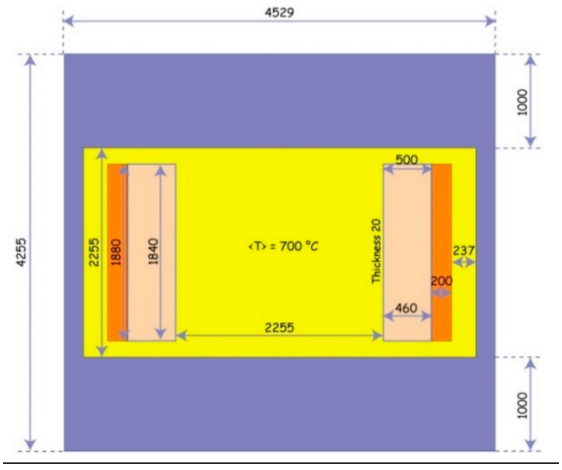

Figure 9: Core model as utilized in simulations (dimensions given in mm) The only things of note here are the yellow sections for the fuel salt and the blue sections for the exterior walls

Instead of modeling the 16 separate fuel loops mentioned in section 2.1.1, the geometry is simplified as a single primary loop that consists of the core, a pipe connecting the core to a single heat exchanger, and a pipe connecting back to the core as depicted in Figure 10,

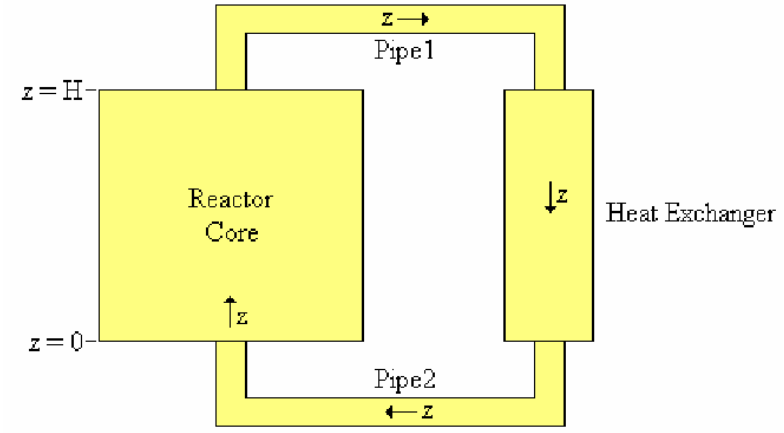

Figure 10: Simplified geometrical model of the MSFR used in the computational model

As a result of the simplification, there is a lack of data characterizing the heat exchanger's geometry and the pipelines that connect it to the reactor core. However, because this is the same model as the one used in [4] for the MSR, the exact approximations will be applied.
Now that only the total volume of fuel salt and the volume present in the core is known, the volume of the two pipes linking the core to the heat exchanger can be determined by estimating the length of each component and assigning each component a uniform circular cross-section.
To further simplify the model, we assume that the molten salt flow field is not radially dependent and that the flow is constant over time. This simplification implies that the code's space-dependent functions can be regarded as constant in the radial direction.

Plug flow is assumed to ensure that the fuel-salt flow velocity does not vary radially. Interaction in the axial direction z is independent of the radial position, and all equations could be represented solely in terms of their axial position z. Because the fuel is moving in an MSFR, the nuclides are also moving, as is shown in the burnup matrix in Figure 6, in order to keep track of the number of nuclides inside the system at each position, the neutron flux $\Phi[z]$ is required.

3.0.2 Neutron Flux

At a given location, the neutron flux is defined as the number of neutrons traveling through an area per second [neutrons cm^{-2} s^{-1}]. A higher neutron flux in a certain area means a greater possibility of neutron-nuclide interaction and a larger number of fission reactions. However, the flux in the core is not taken to be constant. At the reactor core's boundary, neutrons can only come from one direction, as they are formed exclusively within the reactor core, whereas in the core's center, neutrons will come from all directions. Thus, the neutron flux will be greater near the reactor core's center than at its boundary. In a homogeneous cylindrical reactor core, the z-component of the neutron flux has a sine shape [4] This shape is given by:

$$f_{notnormalised}(z) = sin\Big(\frac{\pi(z + 0.5\lambda_{ex})}{H_{ex}}\Big) \tag{14}$$

In this equation, z is the position in the core, H is the height of the core, H_{ex} the extrapolated height of the core, and λ_{ex} [4] is the distance from the core boundary. This value is present in the formula to assure that the flux does not go to zero at the edge but rather at a distance lambda from the edge as showing in Figure 11 below. Additional information can be found in Appendix

B.1.

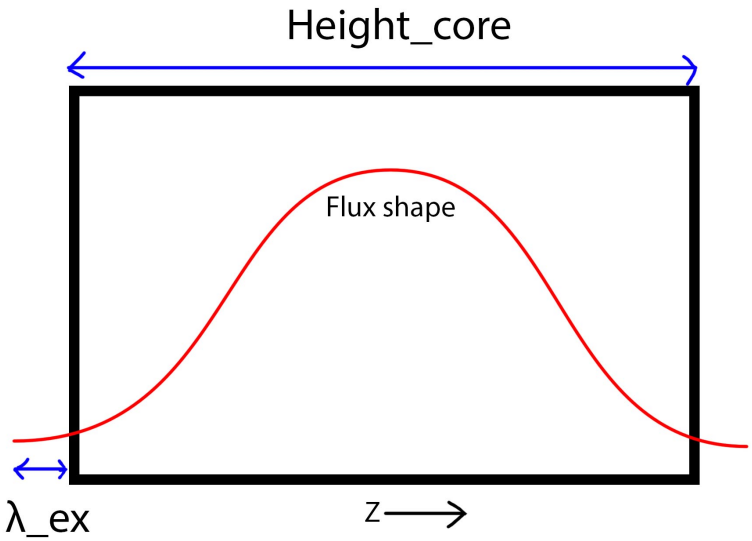

Figure 11: Visualisation of extrapolated lambda and flux shape in core

Equation 14 is normalised, in accordance with [4], as:

$$f(z) = \frac{sin\left(\frac{\pi(z+0.5\lambda_{ex})}{H_{ex}}\right)}{\int_0^H sin\left(\frac{\pi(z+0.5\lambda_{ex})}{H_{ex}}\right)dz} \tag{15}$$

However, Equation 15 has to be discretized in order to be used in the simulation. This is done by replacing the definite integral with a summation to get:

$$f_j = \frac{sin\left[\frac{\pi(z_j+0.5\lambda_{ex})}{H_{ex}}\right]}{\sum_0^H sin\left[\frac{\pi(z_j+0.5\lambda_{ex})}{H_{ex}}\right]\Delta z} \tag{16}$$

The actual curve from Equation 15 and the discredited curve from Equation 16 are both plotted in Figure 12 below:
In order to accurately determine the area under the actual curve using the discretized flux shape, the midpoint rule for Riemann's sum is used.

3.0.3 Flux Weight Factor

The shape of the flux in the core has now been established but lacks the correct amplitude. To solve this, the flux shape has to be multiplied by a weight factor such that:

$$\Phi_j = cf_j \tag{17}$$

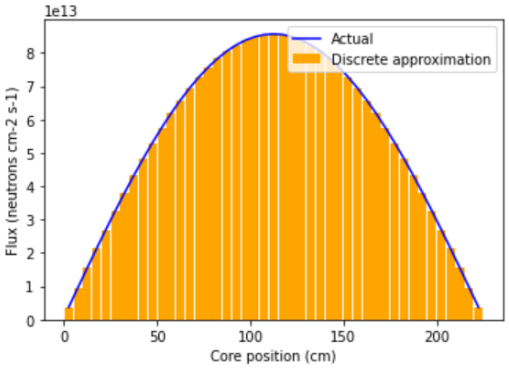

Figure 12: Actual and discrete approximation of unweighted curve of the Neutron Flux Distribution within the core with a $\Delta z = 5$

Where c is the weight factor, f_j the flux shape, and Φ_j the flux at position j in the core.

This weight-factor will be derived in a couple of steps, starting with the equation that describes the thermal power generation of a reactor [10]:

$$P = \sum_k N_k \sigma_{f_k} E_r \Phi V \tag{18}$$

In this equation, N_k is the density of nuclide 'k', $\sigma_{f,k}$ is the fission cross-section of nuclide 'k', Φ is the Neutron density flux, V the volume in the core and E_r is the average recoverable energy per fission (MeV / fission) and is taken as 200 MeV [10]. While it is true that every type of nuclide releases a different amount of energy per fission reaction, these differences are small enough for this estimation to suffice.
It is easy to see that this equation makes sense. The number of nuclides in a specific volume that can fission is considered, along with the likelihood that they fission given by the flux and the energy released through each fission.
In order to conform Equation 18 to our discretized system so that calculations at every z segment can be done, it is written as:

$$P_{tot} = \sum_j P_j = \sum_j \sum_k N_k \sigma_{f_k} E_r A \Delta z \Phi_j = \gamma \sum_j \Phi_j \tag{19}$$

The total power is now calculated by adding the power contribution of each segment within the core. All the z-independent variables are taken out of the summation and substituted by γ for readability on the right side of the equation. The weight factor can now be calculated by combining Equations 17 and 19 such that:

$$\sum_j \Phi_j = \sum_j c f_j = \frac{c}{\Delta z} \sum_j f_j \Delta z = \frac{P_{tot}}{\gamma} \tag{20}$$

Due to the normalization in Equation [16], $\frac{c}{\Delta z} \sum_j f_j \Delta z = 1$ and Equation 20 can be rewritten into an expression for the weight factor:

$$c = \frac{P_{tot}}{\gamma} \Delta z \tag{21}$$

As previously mentioned, the MSFR concept is designed for a nominal power of 3 GW. With that, there is enough information to find the weight factor and calculate the weighted neutron flux density as given in Figure 13

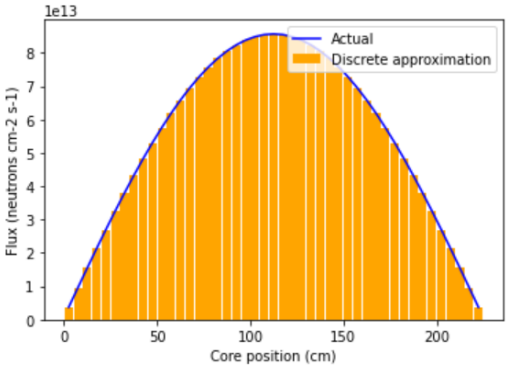

Figure 13: Actual and discrete approximation of weighted curve of the Neutron Flux Distribution within the core with a $\Delta z = 5$

3.1 Implementation In Python

This section will cover the implementation of the theory into Python in order to simulate the equations discussed in Chapter 2. The code is divided into multiple sections: Constants, Nuclides, Flux, Production matrix, and Convection matrix. These parts are then combined and discussed in the section of the Burnup matrix. Properties like the change in nuclide density over time and space or power generation are calculated as well. The code was written to be altered and extended in the future for future study. The most relevant sections of the code will be explained in some more detail below.

Constants

The defined constants include the time over which the reactor is simulated, the dimensions of the system, the positions within the system where nuclides can be inserted or extracted, and the flow rate of the system.
The entire fuel-salt flow loop of the MSFR (core, pipes, and heat exchanger) was spatially discretized by dividing it into volume elements with a uniform length in the z-direction of z and a volume of $A_j \Delta z$, where A_j is the cross-sectional area of an element j perpendicular to the z-axis through which the salt flows. Steps = (Length$_{Core}$ + Length$_{Pipe1}$ + Length$_{HeatEx}$ + Length$_{Pipe2}$) / Δz gives the number of segments the system is divided into.
Length$_{core}$ is the core's height (in cm), Length$_{Pipe1}$ and Length$_{Pipe2}$ are the lengths of the pipes connecting the top of the core to the heat exchanger and the heat exchanger to the bottom of the core, respectively, and Length$_{HeatEx}$ is the heat exchanger's length. All these parts can be seen in Figure 10 above, and the data used for them found in Table 5.

Nuclides

In order to simulate the change of many different nuclides over time and space, a Python class was created. This way, many nuclide-specific properties (e.g., cross-sectional values, atomic weight, initial densities, and decay constants) can be assigned. Defining the nuclides like this makes it easy to add new nuclides or change the properties of existing ones when the simulations have to be extended for future use. The nuclide data is then used to calculate the weight factor for the flux.

Flux

How the total neutron flux is calculated has been explained in Section 3.0.2. Because of some approximations, the flux is only taken nonzero in the core and taken zero outside of the core as shown in Figure 14

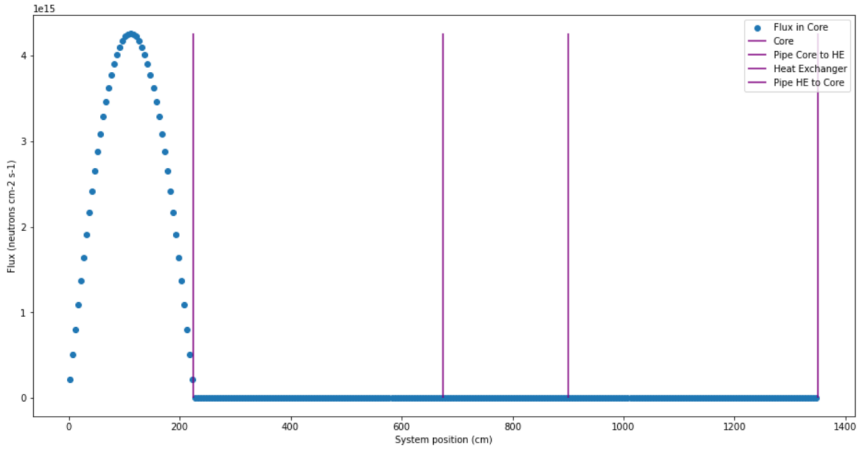

Figure 14: Flux values given at every system segment

Each system segment has a particular flux value assigned to it, and the cross-sectional values, decay constants, and atomic weights for each nuclide are available. This is all the data needed to create the production matrix.

Production matrix

The method by which the production matrix is constructed, as given in Equation 7, is explained via the flowchart in Figure 15.

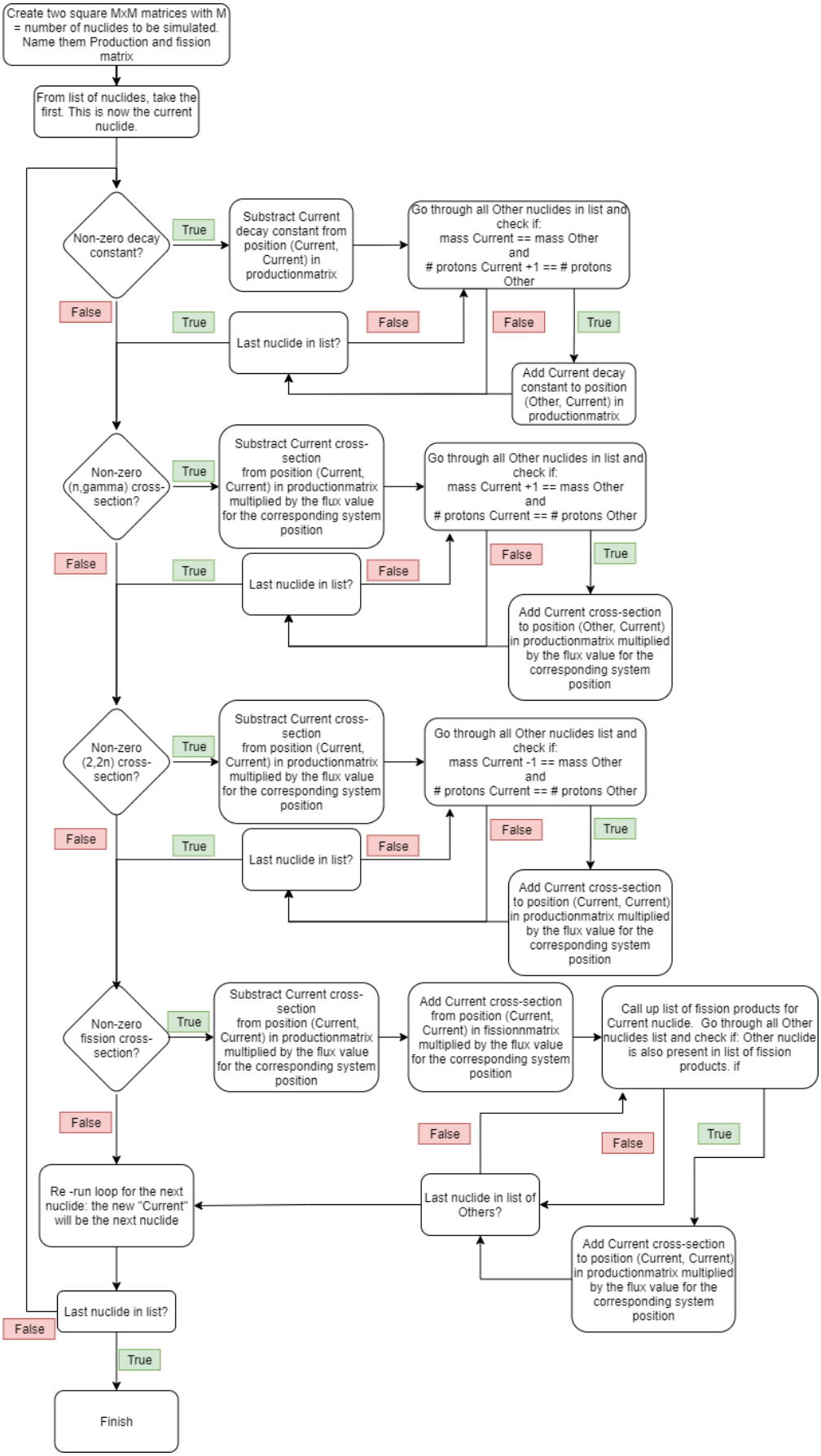

Figure 15: Flowchart explaining the construction of the production matrix within the code

The first nuclide is taken from the list of nuclides and then considered whether it can beta decay and which other nuclides can beta decay into this first nuclide. Take ${}^{232}_{90}Th$ for example. It does not have a decay constant as it is nearly stable. So it will not lower in concentrations due to beta decay. There are also no other nuclides present in this simulation that can decay into ${}^{232}_{90}Th$. Therefore its concentration can only change through neutron-nuclei interactions. How the nuclide concentrations will change exactly will be considered in Chapter 4.

Convection matrix

In order to construct the convection matrix, a formula for the spatial dependent convection terms is created first. These terms had the shape of $\frac{g(t)}{A_j \Delta z}$, and are calculated for every position 'j' in the system: (Core, Pipe1, HeatEx and pipe2). To get an idea of how the convection terms change throughout the system, a Figure is inserted below:

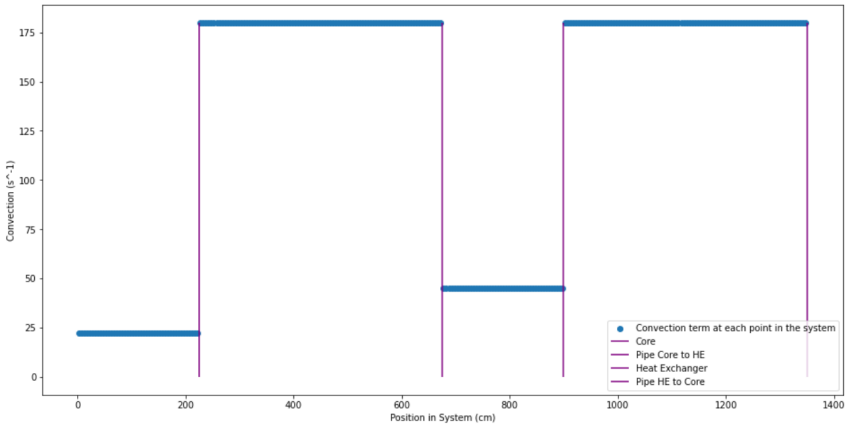

Figure 16: The Convection terms plotted as function of the area and position within the system

The convection matrix starts as an empty matrix with $N * N$ dimensions, with N being the number of nuclides multiplied by the number of segments the system is divided. From the diagonal, the z dependent Convection terms are subtracted. Then, for every column, the z dependent Convection terms are added M places below the diagonal where M is the number of nuclides. Such that Equation 11 is created.

Burn-up matrix

The burnup matrix is created by inserting the production matrices, calculated for each system segment, into the convection matrix at the correct positions as shown in Figure 6. With the burnup matrix created, the next section of the code can be established.

3.1.1 Forward Calculations

Now that all the equations from Chapter 2 have been modeled, the forward calculations can be performed using the explicit Euler method. This is done by rewriting Equation 13 into:

$$C_{k,j}[t+1] = (\Delta t A_j + I) C_{k,j}[t] \tag{22}$$

If the initial density is known, the densities at any time point can be calculated. Here I is the identity matrix, $C_{k,j}[t]$ is the current density of a certain nuclide in a certain position 'j' and $C_{k,j}[t+1]$ the density at a time Δt later.

Nuclide Density

Using Equation 22 with the burnup matrix, a large array containing all the nuclide data is created. The necessary values are extracted for the nuclide density over time and space.

Power Generation

A fission matrix is created along with the production matrix as is seen in Figure 15. This is done to keep track of the number of fission events per volume segment of the system. Summing over the core's entire volume, the total number of fission events can be calculated over time. The reactor's thermal power output can be calculated using Equation 18.

3.2 Reactor Composition Over Time and Space

Simulating the reactor composition over time and space in a realistic way turned out to be quite complicated. These complications have much to do with the relevant time spans for the system. For this reason, we will first discuss time simulation for the production term in the burnup matrix.

Time step size of production

In the simplified simulated thorium cycle, a timespan of around 1000 days has to be considered in order to see a significant change in the number of nuclides within the fuel [11]. As the forward calculations are done with the explicit Euler method, it is essential to keep the time steps sufficiently small to prevent the calculation from diverging into infinity. Nevertheless, as there is little change in this scenario, a step size of 1000 seconds can be used (as was done in [11]). Now that an appropriate time step size, in the order of 10^3 seconds, for the production term is found, the time step size for the convection term can be considered.

Time step size of Convection

To determine the relevant timespan of the convection term, the time it takes for the fuel to circulate once through the system has to be considered. The system's total fuel salt cycle time can be found at the end of the appendix and gives a value of 4.0 seconds. If the time step size found in Section 3.2 is chosen, the fuel will circulate 250 times through the system every time step. Now it becomes clear why simulating both time and space is not a straightforward task.

The convection term represents movement between neighboring segments, which means that the relevant time span is determined by transport time between the segments. The fuel speed varies as a function of the cross-sectional area of the system. The highest fuel velocity is reached in the pipe, so the lower limit for the time span can be found there. The area for the pipes is found in Table 5 in the appendix and has a value of $5 * 10^3$ cm^3. With a flow speed of $g = 4.5 * 10^6$ cm^3 per second, the velocity in the pipes is 900 cm per second. The time it takes for a unit of fuel to move through a system segment that is $\Delta z = 25$ cm long is $27 * 10^{-3}$ seconds.

We therefore found that the relevant time step sizes of the production and convection terms differ by a factor of around $4 * 10^4$. To accurately model the MSFR behavior, we must take the smallest relevant time scale, which is that of the convection term.

Time scale difficulties

We run into some simulation problems when simulating of the rather long time span of 1000 days. Theoretically, taking the smallest time scale as a Δt should pose no problem. However, with a total time span of 1000 days, simulation requires an enormous amount of time steps and uses a lot of memory, making it impossible to simulate the entire process with the current setup. It is possible to use smart vectorization and Python data cropping to make the simulation work, but this is beyond the scope of this thesis. For this reason, two different scenarios are simulated. The first one does not simulate fuel transport and uses all the nuclides from the simplified thorium fuel cycle. The second one aims only to demonstrate the workings of the transport and uses a small number of fabricated nuclides to make it computationally feasible.

3.2.1 Simulation without Convection

It makes no physical sense to use the step size of the production term for simulating the system, as convection can not be accurately modeled with a Δt of 10^3 s. And since the current code cannot simulate the system using the step size of the convection term, the system is first simulated without nuclide transport. Simulating the system without transport gives an indication of weather the interactions between nuclides within the simulated system align with what is expected from the literature. First an upper limit for the time steps had to be found using iteration, because when the time step is taken too large, the code crashes as the explicit Euler method results in a divergence of the nuclide density. With this upper limit the system can be simulated and data can be extracted as will be reviewed in the next chapter.

3.2.2 Simplified Simulation with Convection

In order to show that the code is capable of simulating fuel transport, Figure 17 shows a number of fictional nuclides that have been created based on a few nuclides from the simplified thorium fuel cycle with decay constants similar to the six delayed neutron precursors groups. This way the total simulation time is kept low (30 seconds), allowing for very small time steps to be used whilst still being able to run the code without running out of memory or crashing. Then some of the nuclides have been given cross sectional values in order to simulate neutron-nuclide interaction to make full use of the capabilities of the code. The values assigned to these nuclides can be found in table 6 in the appendix. The cross sectional values for these fictional nuclides had to be chosen in such a way that both effects from beta decay and nuclide-neutron interaction could be observed in the small simulation window.

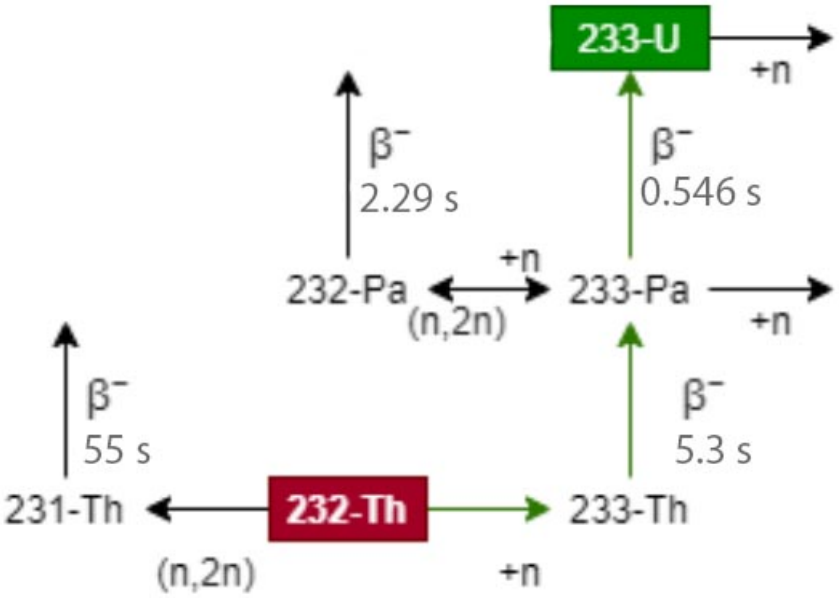

Figure 17: Fictional nuclide decay diagram based upon the simplified thorium fuel cycle

With the simulation parameters setup like this it should be easier to explain what is happening as opposed to using more randomised parameters. If this is indeed the case will be discussed in the next chapter.

3.3 Model Uncertainties

The model uncertainties are to be considered to appreciate the workings of the models used to simulate the behavior of the MSFR fuel composition. The physical values used in the simulations can be found in Appendix B.1. The microscopic cross-section data used of the nuclides are found in Table 4 are taken from a Liquid Metal Reactor. Since this is also a fast reactor design, it is expected that these data are sufficient in simulating the behavior within the scope of this thesis. However, there will be differences between the observed and anticipated values in the data.
Additionally, both the cross-sections and the fission yields are highly dependent on the distribution of the neutron energies. A more accurate system would be able to model these changing values over time. However, correct energy distribution statistics and the range of cross-section and fission yield dependence on this distribution are unavailable and would fall outside the scope of this thesis.
The equation for the neutron flux density is taken as static over time as it is only based on the densities initially present in the system. It would be more accurate to have the flux shape update at every time step as a function of all the nuclides present in the core at that time step.
Additionally, thermodynamics and heat transmission must be considered to present an accurate model of an MSFR. These fields, however, are not addressed in this thesis's reduced simulation. As a result, this thesis is only suited to provide insight into how a fast reactor operates.

4. Results and Discussion

In this section, the results of simulations are given and discussed, starting with how the reactor composition changes over time. The convection terms have been left absent for the first half of this chapter as the simulations could not be calculated whilst simulating the convection term. However, to model the systems convection properly, a simplified system has been simulated in the second part of this chapter using neutron precursor groups that have been modified to be able to undergo neutron nuclide interaction. In the last section of this chapter the system will be simulated over a much longer time to give some more insight in how this simulated reactor compares to the literature.

4.1 Results simulation without Convection

As discussed in Section 3.2, the first solution to the time scaling problem was to use the time scale relevant for the production term. This was found to be $3.3 * 10^3$ seconds.

The reactor composition can be plotted in a couple of different ways using the initial densities given in Table 2 from the appendix; firstly, the change in density of a single nuclide type (e.g., Th-231) at different times over the length of the whole reactor will be simulated. As is illustrated in Figure 18

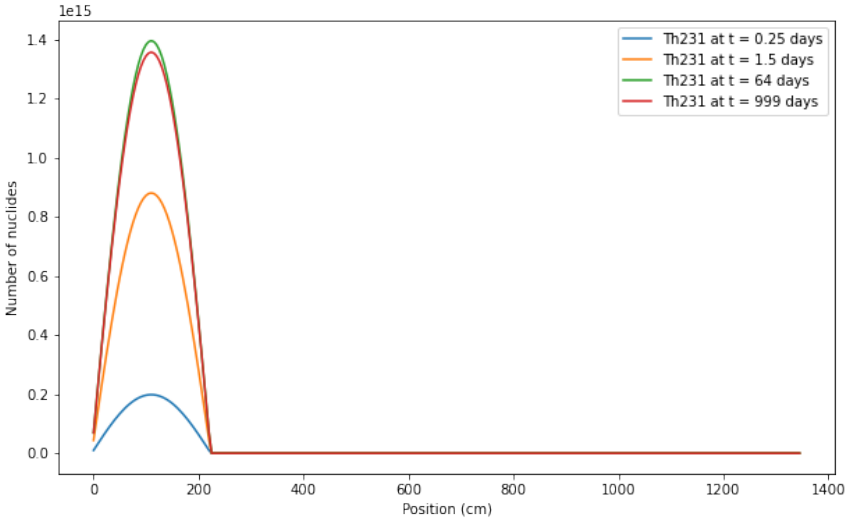

Figure 18: Nuclide density graph of Th231 through the system at a multiple time points over 1000 days

It is interesting to see that the density of Th231 changes relatively quickly within the first couple of days but then slows down and reaches equilibrium. By looking at the properties of Th-231 it can be seen that it is created by Th-232 through a (2,2n) reaction and has a half-life of 25 hours. Equilibrium is formed when decay and production balance out at around the 64 day mark.

Instead of simulating the behavior of a single nuclide type, many different nuclides over the whole length of the system can be simulated as shown in Figure 19. Simulating this will only be done for a single time point as doing this for multiple as done in Figure 18 clutters the graph and impairs readability. The data is plotted using a log scale to more clearly show the changes in all of the nuclides.

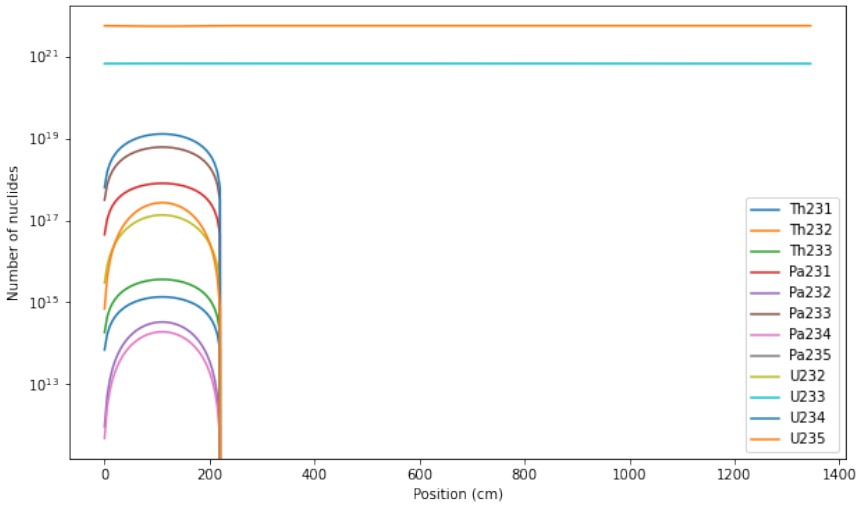

Figure 19: Nuclide density graph of many nuclides through the system at a multiple time points over 1000 days using a log scale on the y axis

After comparing graphs simulated at different time points, it seemed that the one at the 1000 day mark was the most interesting, as it depicts the most prominent change in nuclide concentration within the core. Even so, it is hard to see a change in the two initially present nuclides in Figure 19. Section 4.3 of this chapter will go into more detail.
Looking at Figure 7 it can be seen that the initial nuclides Th232 and U233 only change into other nuclides via neutron-nuclide reactions as they cannot undergo beta decay. This means that only in the core where there is a flux present do other nuclides form. This is what can be seen in Figure 19. This aligns with expectations as there is no fuel transport simulated to move nuclides present in the core to others parts of the system.

In Figure 20, the nuclide densities at the center of the core are plotted over time.

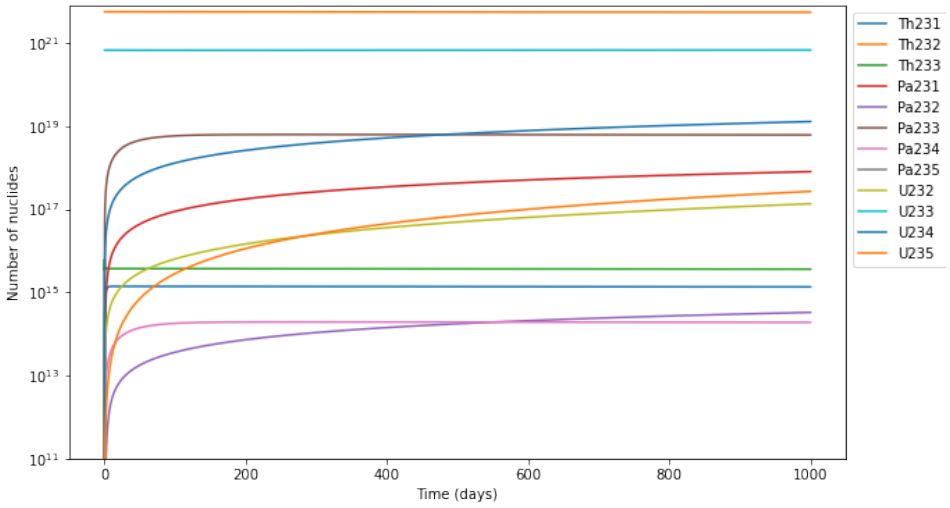

Figure 20: Nuclide density graph of multiple nuclides against the time at a the centre of the core using a log scale on the y axis

With the initial densities in the system taken from Table 2 in the appendix. Figure 20 shows the change in densities of the actinides using the forward equation over 1000 days.
According to this figure, the densities of the initially present nuclides Th232 and U233 barely changes over the 1000 day period.
The nuclides with no initial density are now analyzed using Figure 20 once more again using the simplified thorium fuel cycle in Figure 7 to make sense of the simulated densities over time. Looking at the Protactinium isotopes, two reasons can be given why Pa233 is the most common actinide. The first is that Pa233 has a significantly longer half-life that the other Protactinium isotopes. The second is that when the initially plentiful Th232 undergoes neutron capture, it transforms into Th233 which, with a half-life of around 22 minutes, quickly decays into Pa233. Pa233 increases in concentration up until around the 100 mark here it plateaus as the increase and decrease equal each other. Here the the nuclide is mostly formed by the decay of Th233, and the reduction in density is primarily caused by the beta-decay into U-233.

Pa-231 is another common protactinium isotope. Although it is generated at a lower rate than Pa-233, Pa-231 progressively accumulates over time rather than achieving equilibrium. This can be explained by the fact that Pa-231 has a considerably longer half-life than the other protactinium isotopes.

Note that the uranium isotopes progressively accumulate over time. This is due to their long half-life compared to the 1000 day simulation period
In Section 3.2 it was mentioned that the 1000 days was just an estimate, and therefore we will explore longer simulation times in Section 4.3 to understand how the initially present nuclides will react away.

4.1.1 Power Generation

Considering the thermal power generated by this system, as shown in Figure 21, might be of use in answering why the nuclide densities change so little over the 1000 day period.

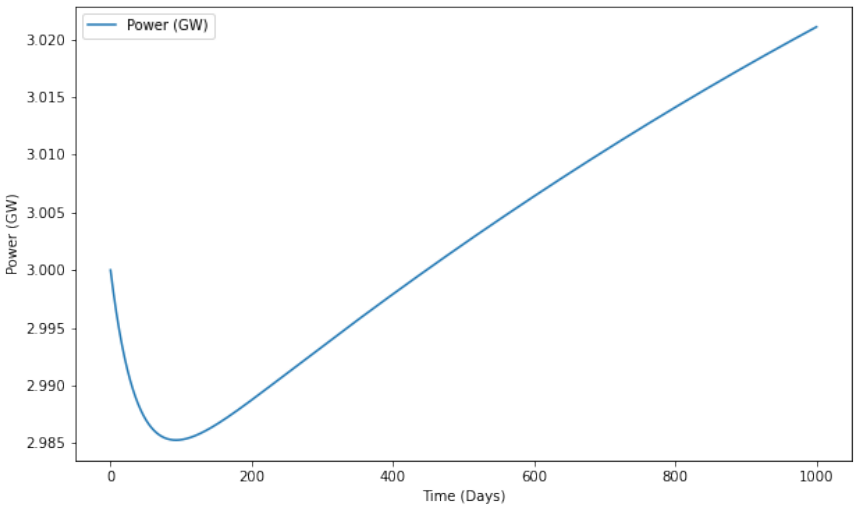

Figure 21: Simulation A: Thermal power generated in core over a 1000 day period

The power starts expectantly at 3 GW, as the flux has been defined with the initial densities of the system. The thermal power output of the reactor is still increasing at the 1000 day mark, which confirms that nuclides have not finished reacting and need more time to do so.

Some things to consider when evaluating the accuracy of this figure. It might be that the cross-sectional values are too small because they were taken from the data for a Liquid Metal Reactor and therefore might not be accurate for an MSR. It is also possible that the neutron flux density ($8e13$ at the center of the core as shown in Figure 12) is too low as it is defined once in the beginning of the simulation and stays static instead of changing in accordance with the fuel composition. Lastly, it might be that this simulation is, in fact, representative of reality.

4.2 Results simplified Simulation with Convection

This part of the discussion will be dedicated to showing that the code does support convectional simulations. Six fictional nuclides based upon the simplified thorium fuel cycle are simulated below over a 30 second time span. The simulation time is kept short in order to run the code with enough spatial and temporal precision.
In Figure 22 a single fictional nuclide based on a Th231 nuclide is simulated on four different time points against the position within the core.

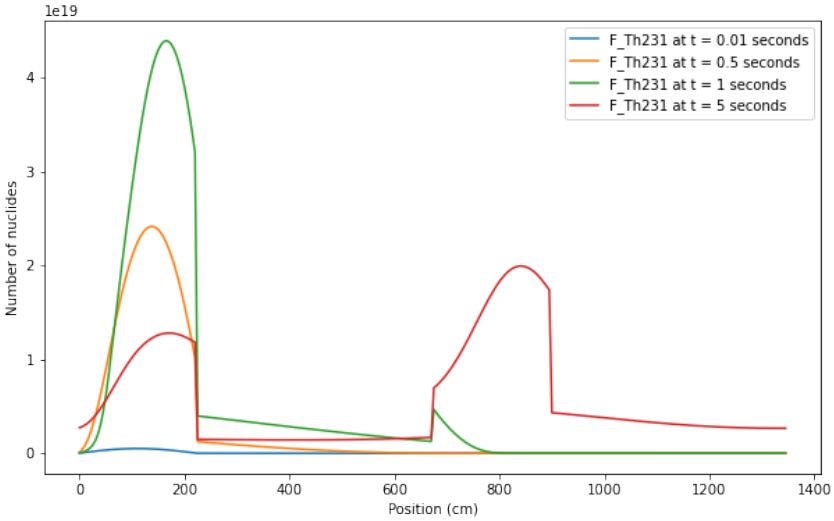

Figure 22: Single fictional nuclide density simulated at four different time points against the position within the reactor

To interpret the results the densities of fictional nuclide F-Th231 care considered for each time point.

At 0.01 seconds in the simulation the only place where F-Th231 exists is within the core with a peak in the center of the core. This is expected as it is created by F-Th232 via an (n,n2) reaction which can only occur within the core. The peak at the center corresponds to where the neutron flux density is highest as shown in Figure 14.

At 0.5 seconds the density of F-Th231 has risen compared to the previous point. Not much of the newly created F-Th231 has flowed out of the core yet. This is expected as it takes 4.1 seconds for the fuel to flow through the system once. And almost none has reached the heat exchanger as of yet.

At 1 seconds into the simulation the density of F-Th231 peaks as now a large amount is produced within the core. It can be seen that a somewhat steady flow is of nuclides is on its way to the heat exchanger through the first pipe. The flow there has still not balanced out yet as there is a higher density at the beginning The small spike in concentration at the beginning of the heat exchanger is expected to be seen as the flow speed at that point suddenly deceases due to the larger area of the heat exchanger.

At 5 seconds the fuel has already completed a full cycle through the system. The previous peak within the core has flattened somewhat as the fuel homogenises through the system and as it decays away. When running this simulation for later times it becomes more apparent that F-Th231 decays away even though its half-life is long with respect to the total simulation time. The density within the heat exchanger seems to be increasing towards the right. This cannot be the result of a nuclear reaction as there is no flux present there. It might be due to how the fuel behaves as it transitions from a fast to slow flowing area as more fuel comes in the density

keep increasing until it flows out into the fast flowing second pipe. Furthermore, the flow in the second pipe seems to have stabilised at this time as the beginning and end of the pipe have around the same amount of F-Th231

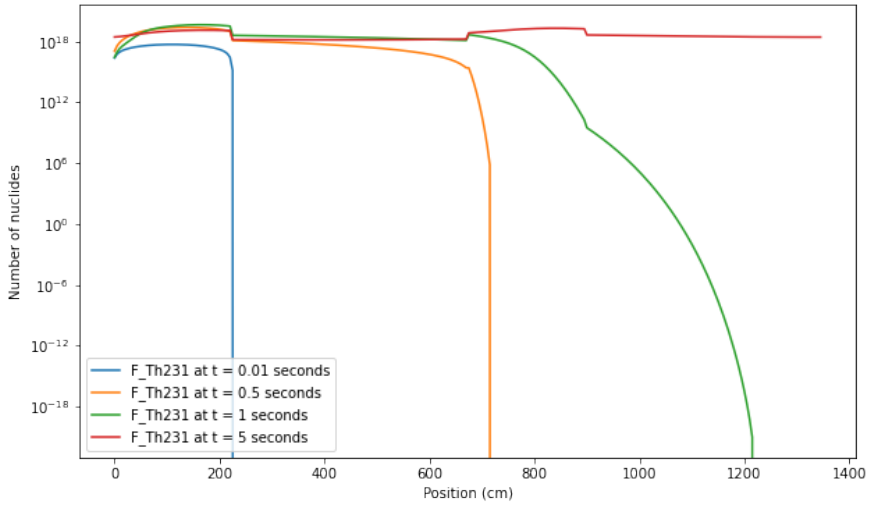

Figure 23: Single fictional nuclide density simulated at four different time points against the position within the reactor using a log scale on the y axis

F-Th231 has no initial density in the reactor. Figure 17 shows how F-Th231 is created by F-Th232 via an (n,n2) reaction and beta decays away over 55 seconds. Considering that the simulation only runs for 30 seconds we expect the concentration of F-Th231 to stabilise as it has the longest half-life of any of the fictional nuclides. Figure 23 seems to confirm this where the density change is easier to read in a logarithmic scale.

Figure 24 now shows all the fictional nuclides simulated at the 5 second mark over the length of the reactor.

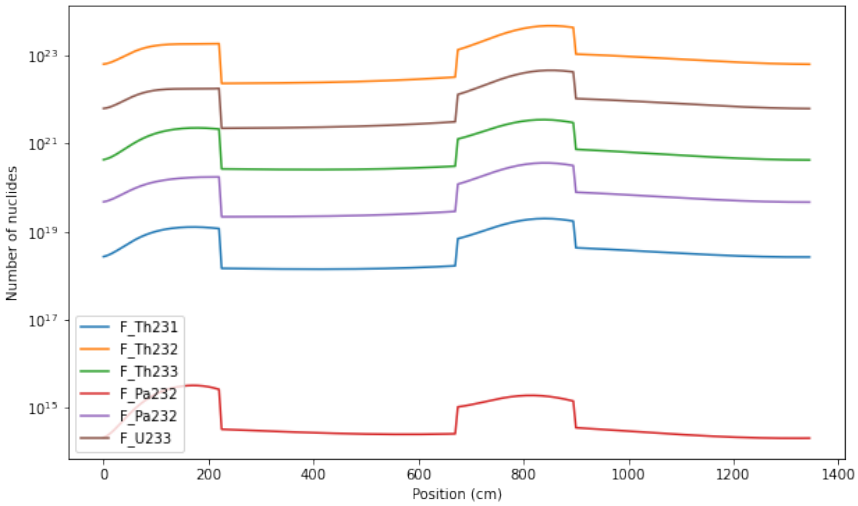

Figure 24: All the fictional nuclide densities simulated at the 5 second mark against the position within the reactor using a log scale on the y axis

In Figure 24 it can be seen that all nuclides follow the same pattern as described for Figure 22 at the 5 second mark. Sharp increase in density at the transition point between a fast and slow flowing area. As well as the gradual increase in density in the slow flowing areas (core and heat exchanger). The differences in concentration are a result of the specific properties of each fictional nuclide and how these affect the production and decay of each.

Figure 25 depicts the change in the fictional nuclide densities measured in the center of the core over the total simulation time of 30 seconds.

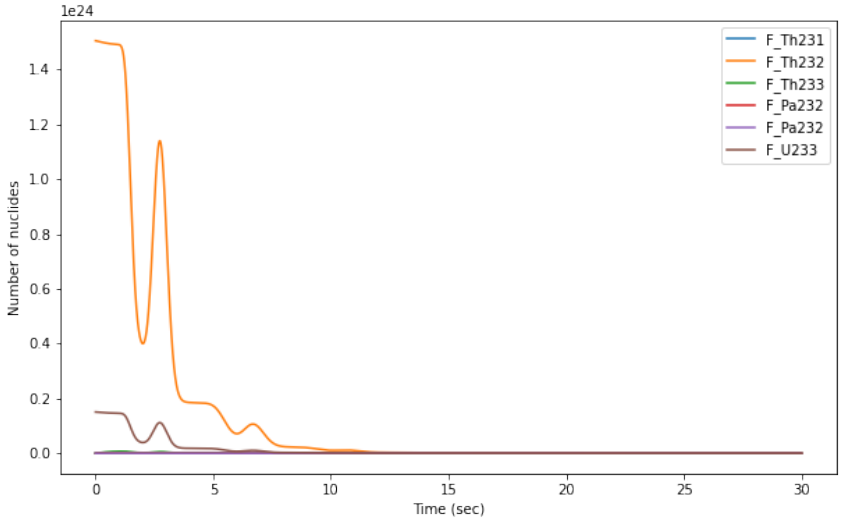

Figure 25: All the fictional nuclide densities simulated at the center of the core over a period of 30 seconds

The two fictional nuclides with initial densities, F-Th232 and F-U233 seem to slowly react in the first second within the core after which they sharply decrease, followed by an increase and subsequent decrease. After the fuel has made one, 4.1 second, cycle this behavior seems to repeat itself.

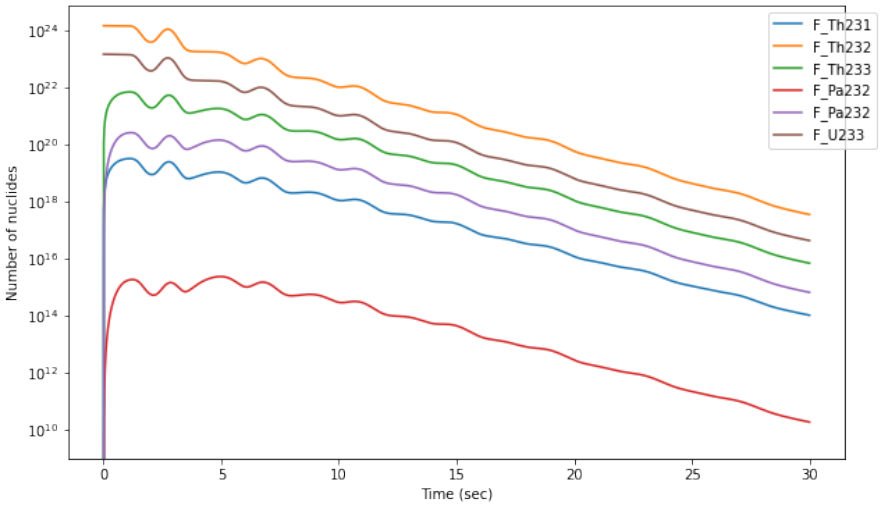

Figure 26: All the fictional nuclide densities simulated at the center of the core over a period of 30 seconds using a log scale on the y axis

Figure 26 shows the same as Figure 25 above but with log scale on the y axis. Here it can

be clearly seen how, as F-Th232 and F-U233 react, new nuclides are formed within the first moments of the simulation and how all fictional nuclides react away as time progresses. The periodic density fluctuations can be seen here as well as they slowly die fade out.

4.3 Extended Simulation

In this section the reactor operation has been simulated over a time span of 15000 days in order be able to see how long it takes for the nuclides to react away. To achieve this computationally, the spatial accuracy has been reduced five-fold to save on memory used. Over such a long simulation time any errors in initial conditions will have more noticeable impact on the end result.

Something that can be considered is the time it takes for the power output of the system to go to zero. To see how long this should take we can calculate how long it should take for the initially present Th-232 to react away. The total mass of Th232 initially present amounts to 38 metric tonnes when considering the initial fuel composition, total fuel volume and weight of a Th232 nuclide.

There are two ways to calculate the reaction rate of Th232 and with it the amount that reacts every day. One uses the cross sectional values of Th232 to calculate how many nuclides react every day. The other calculates how much Th232 needs to react in order to reach the desired power output of the reactor.
Both these methods are flawed however as the first relies on the flux, which in a more realistic simulation changes with time. The second assumes constant power output where in the simulation it fluctuates. However, since the point of this is to get a rough idea of the amount of time it would take to burn through all the thorium the second method suffices for now. The reactor would burn through 3.11 kg of Th232 per day to maintain a target output of 3GW. This means that it would take 12354 days to burn through all the thorium.

Figures 27 depicts the change in nuclide densities of the system over a period of 15000 days with a neutron flux density increased by factor 50.

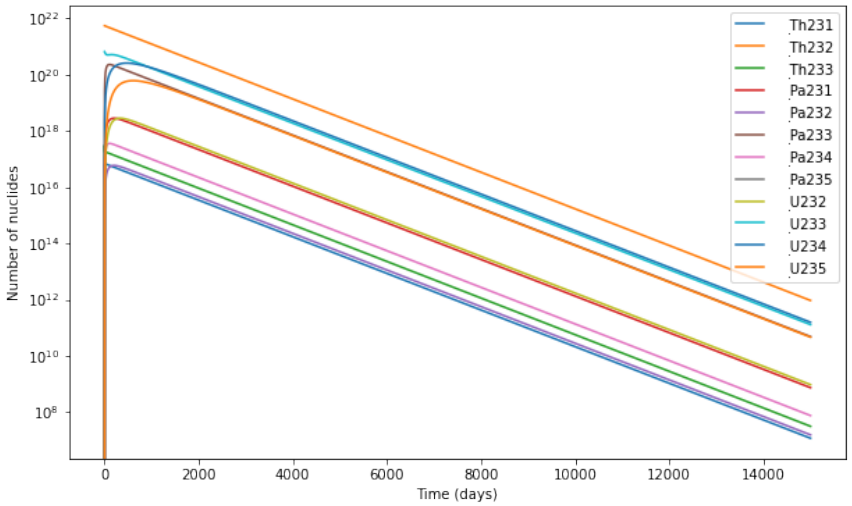

Figure 27: Nuclide density graph of multiple nuclides at a the centre of the core over 15000 days using a log scale on the y axis

Even with the flux multiplied by a factor 50, the Th232 nuclide density did not reach close to zero. There are many possible reasons for this. The calculations made above are inaccurate and should give a larger amount of days for Th232 to react away. Or as mentioned in Section 3.3, the neutron flux density within the system is lower than it should be as it is calculated once using the initial conditions of the system. In which only Th-232 and U-233 contribute to the flux intensity. However, as time goes on Pa-231, U-232, U-234 and U-235 will also contribute to the flux by producing neutrons. A more realistic model would recalculate the flux at every time step.

4.4 Additional Simulations

So far, the fission cross-sections have only been used to calculate the power output of the system. The code has been set-up to also simulate the behavior of the fission products over time. But due to time constraints this has not been simulated and will be left for future research.

5. Conclusion

The goal of this thesis was to model both time and spatial dependence of fuel composition within an MSFR. A simplification of the MSFR was made by modelling only a single primary loop and by assuming no external transport of fuel salts. This gave rise to a system of equations with a convection term and a nuclide production/destruction term. As it appeared, however, the convection term blew up the nuclide densities in the code and therefore two separate simulations had to be done.

The first without a convection term, where all the nuclides from the simplified thorium fuel cycle were present. This model gave an accurate representation of the change in fuel composition. The second a simplified system using fictional nuclides based on the simplified thorium fuel cycle that was aimed purely at showing that simulation fuel transport is indeed possible. As of yet, it is still very inefficient and takes much time to calculate, making it less than ideal when used to learn about the workings of the MSFR.

The explicit Euler method was used to model temporal dependence, which encompassed two different time scales for the two main parts of the system equation. Taking the smaller convection time scale led to a scaling problem, due to the large time span over which the system had to be modelled.

It is obvious that many aspects of this model are still to be improved. Most prominently, smaller time steps are required such that convection can be simulated in the main physically accurate model. These smaller time steps were not possible because they would lead to a scaling problem. In further research, this problem could be overcome by using vectorization to replace many of the for-loops within the model. This would drastically reduce the computation time for the simulation. Moreover, as the model required too much memory when time steps were too high, a solution needs to be found to crop the data. This could be done by using Python packages which store data more compactly, or by plotting the data while the for-loop is running.
After the convection has been successfully implemented, it would be interesting to also model the fission products. Only the fission energy was considered in determining the thermal power output of the system, and modelling the resulting products of these reactions fell beyond the scope of this thesis.

Finally, perturbation theory could be implemented in order to significantly increase the versatility of the reactor model. Perturbation theory assumes that the system quantities only change by small perturbations relative to the total value in the reactor. This makes it possible to simulate how the system changes because of these perturbations, instead of re-simulating the entire process.

6. Acknowledgements

I'd like to express my gratitude to my supervisors, Jan Leen Kloosterman and Danny Lathouwers, for the weekly meetings during which I received guidance and answers to my questions.

Bibliography

[1] Tayo Ajadi, Victoria Cuming, Rohan Boyle, David Strahan, Matthias Kimmel, Michael Logan, Angus McCrone, et al. Global trends in renewable energy investment 2020. 2020.

[2] Olivier Corradi. Live c02 emissions of electricity consumption. `https://www.electricitymap.org/zone/GB?solar=false&remote=true&wind=false`, 2018. Accessed: June-2020.

[3] Energy from Thorium. Documents related to liquid-halide (fluoride and chloride) reactor research and development, 2013.

[4] Gert Auwerda and D. Lathouwers. Computational modeling of a molten salt reactor. 06 2021.

[5] Cordis EU Research results. Evol (project n°249696) final report. Technical report, The European Commission, November 2013.

[6] E Merle-Lucotte, D Heuer, M Allibert, M Brovchenko, V Ghetta, A Laureau, and P Rubiolo. Preliminary design assessment of the molten salt fast reactor. *Proceedings of the ENC2012-Advanced Reactors*, pages 17–26, 2012.

[7] Multiple Authors. Reactor thermal power: Definition amp; values. `https://www.nuclear-power.net/nuclear-power/reactor-physics/reactor-operation/xenon-135/`, Mar 2021. Accessed: June-2020.

[8] Jan Leendert Kloosterman. Actinide data for transmutation studies. 1995.

[9] D Journée. Helium bubbling in a molten salt fast reactor. a flotation process, 2014.

[10] Multiple Authors. Reactor thermal power: Definition amp; values. `https://www.nuclear-power.net/nuclear-power/reactor-physics/neutron-diffusion-theory/reactor-thermal-power/`, Mar 2021. Accessed: June-2020.

[11] F Pauwels. Burnup simulations of the thorium cycle in a msfr using perturbation theory, 2020.

[12] Iwamoto Osamu. Fission yield graph. `https://wwwndc.jaea.go.jp/cgi-bin/FPYfig`, 1995. Accessed: June-2020.

A. Appendix

B. Definitions

Thermal Neutrons
Neutrons in thermal equilibrium with the medium in which they exist. At 20°C, the most likely energy is $0.025eV$ (2200 m/s). This portion of the neutron's energy spectrum is the most important in thermal reactors.

Fast Neutrons
Neutrons with a kinetic energy greater than 1 MeV (15000 km/s). Fast neutrons are slowed down to thermal energies inside a thermal nuclear reactor through a process called neutron moderation.

Fuel Salt
Molten salt reactors (MSRs) are a type of reactor that use liquid salt, typically fluoride or chloride-based, as a coolant and fuel in combination, with the fuel dissolved in a carrier salt.

Criticality
In nuclear reactors, reactor criticality refers to the state of a reactor that is stable and capable of self-sustaining nuclear chain reactions. This state is also referred to as the critical state.

Enrichment
Uranium enrichment is a process that increases the percent composition of uranium-235 via isotope separation. The level of enrichment required varies according to the type of reactor, with fast reactors requiring a higher level of enrichment than thermal reactors.

Fission Products
Nuclear fission products are the atomic fragments that result from the nuclear fission of a large atomic nucleus. Typically, a large nucleus such as uranium fissions by splitting into two smaller nuclei, releasing heat energy (the nuclei's kinetic energy), and gamma rays. The two smaller nuclei are the result of fission.

Micoscopic Cross-section
The microscopic cross section is the effective target area presented by a single nucleus to an incident neutron beam.

Neuron Flux Density
The neutron flux density is the number of neutrons passing in all directions through an arbitrary cross-sectional unit area per unit time. It is a scalar quantity that can be calculated by multiplying the neutron density by the neutron velocity.

Actinides
The actinides are a group of fifteen metallic chemical elements with atomic numbers ranging from 89 to 103.

Rankine Cycle
The Rankine cycle is a idealised thermodynamic cycle that describes how certain types of heat engines, such as steam turbines, extract mechanical work from a fluid as it moves between a heat source and a heat sink.

Neutron Poisons
Neutron poisons are fission products that cause problems in reactors due to their ability to act as parasitic neutron absorbers, resulting in long-term sources of heat (so called decay heat). Typically, their accumulation in the reactor has a detrimental effect on its operation.

B.1 Data used in simulations

B.1.1 Actinide decay and cross-sectional data

Cross-sectional and decay data for the actinides used in the simulations displayed in table[1] Data taken from a LMR as there is no data to be found for a MSFR

Table 1: Actinide Decay One-Group Cross Sections LMR-MOX [8], [11]

Nuclides	σ_c **(Barn)**	σ_f **(Barn)**	σ_{n2} **(Barn)**	**Half-life (Days)**
Th231	*	*	*	1.063
Th232	0.396	0.011	2.234	*
Th233	*	*	*	0.016
Pa231	2.980	0.258	1.479	*
Pa232	*	*	*	1.312
Pa233	1.056	*	0.612	26.975
Pa234	*	*	*	0.279
Pa235	*	*	*	0.017
U232	0.662	2.264	1.117	*
U233	0.261	2.774	1.137	*
U234	0.602	0.349	0.222	*
U235	0.535	1.906	1.490	*

Cells with * have values that are negligibly small.

B.1.2 Initial Fuel Composition

MSFR initial fuel composition of LiF-ThF4-UF4 corresponding to 77.5, 20 and 2.5 mol percent [6] of total respectively. With a fuel salt density of 4.1 g/cm3.

Table 2: Initial fuel concentration of MSFR given in various units

Salt type	**Molar comp.**	**Mass** ($\backslash\frac{g}{mol}$)	**Mass comp.**	**Density** ($\frac{g}{cm^3}$)	**Concentration** ($\frac{mol}{cm^3}$)
LiF	77.5 %	6.94+19.00=25.94	22.47 %	0.921	0.0355
ThF4	20 %	232.04+4(19.00)=308.04	68.88 %	2.824	0.0092
UF4	2.5 %	233.04+4(19.00)=309.04	8.64 %	0.354	0.0011
Total	100 %		100%	4.1	0.0458

B.1.3 Fission yield

The fission yields are given in products created per 1000 fission events for each nuclide. Given in table[3]. Data from [12]

Table 3: Fission yields for a select number of poisons.

	Th232	**Pa231**	**U232**	**U233**	**U234**	**U235**
Xenon 135	1.39	6.57	17.3	18.2	18.4	14.6
Xenon 136	6.53	21.6	45.6	28.5	34.4	21.8
Tellurium 135	24.5	19.3	6.79	5.20	5.84	10.5
Iodide 135	22.8	40.2	28.3	26.5	29.0	31.5
Cesium 135	0	0	0	1.63	1.45	0

B.1.4 Half-life of Poisons

The half-life of the poisons are listed in table[4]

Table 4: Half-life of poisons

Poisons	β^- **Decay (days)**
Xenon 135	0.380
Xenon 136	Stable
Tellurium 135	0
Iodide 135	0.274
Cesium 135	Semi stable

B.1.5 Reactor Geometry

The extrapolated height of the core is given by :

$$H_{ex} = \lambda_{ex} + H \tag{23}$$

With λ_{ex} thermal extrapolation distance and H the height of the core [Page 49][Weston M. Stacey, Nuclear Reactor Physics, Wiley-VCH, Weinheim, 2004.]. The λ_{ex} in that thesis was used for a core height of the MSR of 200 cm and had a value of 1.95 cm, which resulted in Hex = 201.95 cm. This report models a core height of 225. The λ_{ex} is thus increased to 2.19 cm. Which results in H_{ex} = 227.19 cm.

Table 5: Modeled plant geometry (HE = heat exchanger)

	Height/Length (cm)	**Volume** (cm^3)	**Area (V/H)** (cm^2)
Core	225	$9.00 * 10^6$	$4 * 10^4$
Pipe core to HE	450	$2.25 * 10^6$	$5 * 10^3$
HE	225	$4.50 * 10^6$	$2 * 10^4$
Pipe HE to core	450	$2.25 * 10^6$	$5 * 10^3$

Step size in the z-direction: $\Delta z = 25cm$.
The fuel-salt flow-rate $g = 4.5 * 10^6 \frac{cm^3}{s}$ Total fuel salt cycle time in system = 4.0 sec [5]

Table 6: Table containing the data used to simulate the convection of fictional nuclides.

Nuclides	**Proton Number**	**Atomic Weight**	σ_c **(cm2)**	σ_f **(cm2)**	σ_{n2} **(cm2)**	**Half-life (Sec)**	**Inital Density (mol)**
F_Th231	90	231	0	0	0	55.11	0
F_Th232	90	232	0.32e-15	0.258e-15	1.4e-3	0	2.5
F_Th233	90	233	0	0	0	5.300	0
F_Pa232	91	232	0.496e-15	2.774e-15	0	2.290	0
F_Pa233	91	233	0.2e-15	0.349e-15	1.1e-3	0.546	0
F_U233	92	233	0.05e-15	1.906e-15	0	0	0.25